

UNCLASSIFIED

AD 408 920

DEFENSE DOCUMENTATION CENTER

FOR

SCIENTIFIC AND TECHNICAL INFORMATION

CAMERON STATION, ALEXANDRIA, VIRGINIA



UNCLASSIFIED

NOTICE: When government or other drawings, specifications or other data are used for any purpose other than in connection with a definitely related government procurement operation, the U. S. Government thereby incurs no responsibility, nor any obligation whatsoever; and the fact that the Government may have formulated, furnished, or in any way supplied the said drawings, specifications, or other data is not to be regarded by implication or otherwise as in any manner licensing the holder or any other person or corporation, or conveying any rights or permission to manufacture, use or sell any patented invention that may in any way be related thereto.

④ \$6.60 ⑤ 697 900

④ TR 1948
⑤ 31 December 1962

TECHNICAL DOCUMENTARY REPORT

⑥ DOPPLER TRACKING LOOP
OPTIMIZATION STUDY

Prepared by

PHILCO CORPORATION
Western Development Laboratories
Palo Alto, California

⑦ Contract AF04(695)-113

Prepared for

SPACE SYSTEMS DIVISION
AIR FORCE SYSTEMS COMMAND
UNITED STATES AIR FORCE
Inglewood, California

① NA
② NA
③ NA
④ NA
⑤ IV
⑥ NA
⑦ NA
⑧ NA
⑨ NA
⑩ NA
⑪ NA
⑫ NA
⑬ NA
⑭ NA
⑮ NA

by C

63 1 706

PHILCO

WESTERN DEVELOPMENT LABORATORIES

SUMMARY

The purpose of this study was to investigate methods for improving the performance of the phase-locked loop receiver, particularly as a reliable means for locking onto and determining precisely the doppler frequency shift of a 2-gc carrier in the presence of noise.

Section 1 contains a discussion and an analysis of one particular type of adaptive phase-lock to verify that the theoretical design of the deliverable breadboard can actually be realized in a working model.

The hardware developed for the experimental adaptive selector is described in Section 2, including the two phase detectors, the integrator, the multipliers, the voltage-controlled oscillator, the gate control, the variable pulse width generator, and the sweep generator.

A general analysis of the usual phase-locked loop lock-on procedure is contained in Section 3, showing that, through this procedure is not an optimum method, it is nevertheless a good practical solution.

In Section 4, interference to a tracking loop from an unwanted carrier (with limiting) is discussed, and it is shown that the phase-locked loop is not ideally suited to a secure communication system.

A discussion of doppler loop threshold is contained in Appendix A; two formulations are given for obtaining threshold optimization.

A

ABSTRACT

PHILCO WDL-TR1948
DOPPLER TRACKING LOOP
OPTIMIZATION STUDY
31 December 1962

UNCLASSIFIED

61 pages
Contract AF04(695)-113

The purpose of this study was to investigate methods for improving the performance of the phase-locked loop receiver, particularly as a reliable means for locking onto, and determining precisely, the doppler frequency shift of a 2-gc carrier in the presence of noise.

~~In this report,~~ the following subjects are discussed in detail: adaptive phase-lock theory, receiver description, optimization of phase-locked loop lock-on, interference to a tracking loop from an unwanted carrier (with limiting), and doppler loop threshold.

THIS UNCLASSIFIED ABSTRACT IS DESIGNED FOR RETENTION IN A STANDARD 3-BY-5 CARD-SIZE FILE, IF DESIRED. WHERE THE ABSTRACT COVERS MORE THAN ONE SIDE OF THE CARD, THE ENTIRE RECTANGLE MAY BE CUT OUT AND FOLDED AT THE DOTTED CENTER LINE. (IF THE ABSTRACT IS CLASSIFIED, HOWEVER, IT MUST NOT BE REMOVED FROM THE DOCUMENT IN WHICH IT IS INCLUDED.)

- A -

PHILCO

WESTERN DEVELOPMENT LABORATORIES

FOREWORD

This Technical Documentary Report on Definitive Contract AF04(695)-113 has been prepared in accordance with Exhibit "A" of that contract and Paragraph 4.2.2 of AFBM Exhibit 58-1, "Contractor Reports Exhibit," dated 1 October 1959, as revised and amended.

This report was prepared by Philco Western Development Laboratories in fulfilling the requirements of Paragraph 1.2.1.2 of AFSSD Exhibit 61-27A, "Satellite Control Subsystem Work Statement," dated 15 February 1962, as revised and amended.

TABLE OF CONTENTS

<u>Section</u>		<u>Page</u>
1	ADAPTIVE PHASE-LOCK THEORY	1-1
1.1	General	1-1
1.2	Phase-Locked Loop Theory	1-1
1.3	The Goal	1-3
1.4	The Three Causes of Phase Error	1-4
1.5	The Optimum Design	1-12
1.6	Variable Bandwidth Loop Design	1-15
2	RECEIVER DESCRIPTION	2-1
2.1	General	2-1
2.2	Adaptive Doppler Tracking Detector	2-2
3	OPTIMIZING PHASE-LOCKED LOOP LOCK-ON	3-1
3.1	General	3-1
3.2	Lock-On Procedure	3-1
4	INTERFERENCE TO A TRACKING LOOP FROM AN UNWANTED CARRIER (WITH LIMITING)	4-1
4.1	General	4-1
<u>Appendix</u>		<u>Page</u>
A	DOPPLER LOOP THRESHOLD	A-1
A.1	Threshold Optimization	A-1

LIST OF ILLUSTRATIONS

<u>Figure</u>		<u>Page</u>
1-1	Basic Loop Configuration	1-2
1-2a	Non-Perfect Integrator Loop Dynamics	1-6
1-2b	Dynamics of Loop Stabilized With An Ideal Integrator	1-6
1-3a	Maximum Drift Ratio for the Non-Perfect Integrating Loop	1-8
1-3b	Typical Shape of a Satellite Doppler Rate Curve	1-8
1-4a	Equivalent Loop for Noise Input Only	1-9
1-4b	Signal Loop Where Phase Error is the Output Variable	1-9a
1-5	Relative Noise Bandwidth for an Integrating Filter Type of Phase-Locked Loop of Fig. 1-4a	1-11

LIST OF ILLUSTRATIONS (Continued)

<u>Figure</u>		<u>Page</u>
1-6a } 1-6b }	Two examples Resulting in a Similar Threshold Value	1-13
1-7	The Adaptive Bandwidth Detector	1-16
1-8	Simple Block Diagram	1-17
2-1	Block Diagram of the Detector	2-3
2-2	Phase Detector	2-4
2-3	Integrator	2-6
2-4	Multipliers	2-7
2-5	Voltage Controlled Oscillator	2-8
2-6	Phase Detector	2-10
2-7	Gate Control	2-11
2-8	Variable Pulse Width Generator	2-12
2-9	Sweep Generator	2-13
3-1	Block Diagram of a Typical Loop Sweep and Lock-On Circuit	3-2
3-2	The Ideal Detector	3-7
3-3	The Near Ideal Detector	3-7
3-4	The Error Probabilities for a Single Channel	3-9
3-5	The Optimum Receiver	3-14
4-1	Solving for the Input Phase -- With Limiting	4-2
4-2	Input Phase as a Function of Time ($E_2/E_1 = 0.6$)	4-2
4-3	A Typical Root Locus for Finding the Maximum Phase Error	4-4
A-1	Distribution of Phase Error	A-1

LIST OF TABLES

<u>Table</u>		<u>Page</u>
4-1	Fourier Coefficients of $\theta(t)$	4-3

WDL-TR1948

SECTION 1
ADAPTIVE PHASE-LOCK THEORY

SECTION 1

ADAPTIVE PHASE-LOCK THEORY

1.1 GENERAL

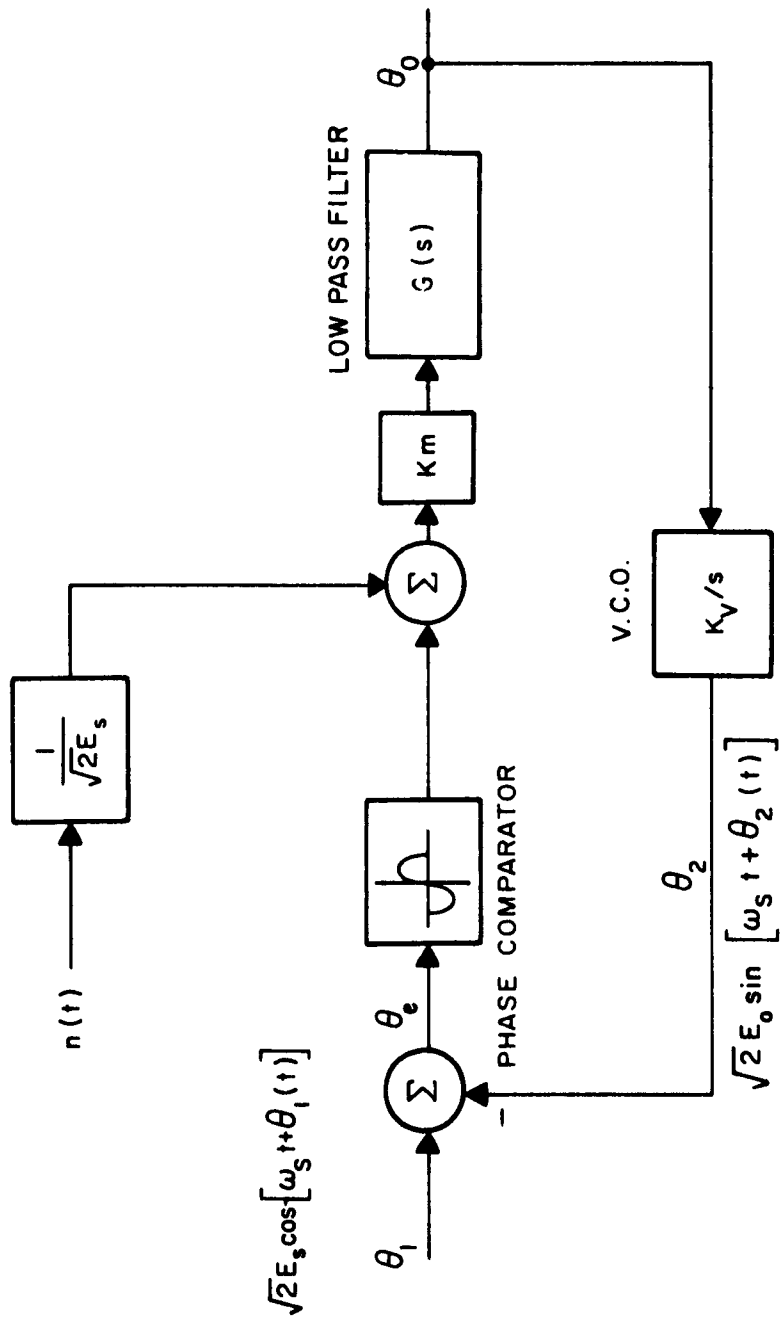
This Section contains a discussion and an analysis of one particular type of adaptive phase-lock to verify that the theoretical design of the deliverable breadboard can actually be realized in a working model. The fundamental rule governing the design objectives in this area is the replacement of the human operator with automatic equipment that will benefit system performance and cause no reduction of reliability.

1.2 PHASE-LOCKED LOOP THEORY

The phase-locked loop is a feedback device which compares the phase of an incoming signal with the phase of a local oscillator. When the phases differ by a constant value of 90 degrees, there is no output from the phase comparator and the loop is said to be perfectly in lock. Any phase difference other than 90 degrees (a phase error) gives a d-c output which is fed back to change the local oscillator (VCO) frequency. The change is made in a direction that will reduce the phase error.

Figure 1-1 illustrates the basic phase-locked loop. The loop is shown with two inputs; one representing the phase of the incoming carrier and the other injecting noise which occurs with the received carrier. This representation emphasizes the role that noise plays in disturbing the loop.

The loop is non-linear because of the phase comparator characteristics. In Fig. 1-1, the non-linear component is shown as being sinusoidal. This description holds as long as the carrier of the two signals entering the phase comparator are both sinusoidal. However, if both signals are square wave or well limited sine-waves, the non-linearity is a repetitive triangular function. In either case, the non-linearity is neglected for small signal analysis.



DWG A12449

Fig. 1-1 Basic Loop Configuration

It is desirable to have the closed loop noise bandwidth as narrow as possible while keeping the signal bandwidth wide enough to allow the loop to follow the doppler rate without excessive phase error.

1.3 THE GOAL

The criterion for optimality in a doppler tracking loop is accuracy in the count of zero crossings of the VCO signal. The VCO is of course locked to the signal in the incoming waveform, but because the actual VCO signal is internally generated, it is less contaminated with extraneous zero crossings.

It has been derived by Stumper¹ that the long term average frequency as determined by counting zero crossings is

$$f_{avg} = \left[f_o^2 + \frac{\Delta f^2}{3} e^{-\rho} \right]^{\frac{1}{2}} \quad (1-1)$$

where f_o is the center frequency of a bandpass filter $2 \Delta f$ wide and containing a single sinewave in noise ($\rho \approx S/N$). For small errors in average frequency (ϵ) it is possible to arrange the preceding equation as a frequency ratio;

$$\frac{\epsilon}{f_o} = \frac{1}{3} \left(\frac{\Delta f}{f_o} \right)^2 e^{-\rho} \quad (1-2)$$

To achieve a small error ratio, the interpretation is straight forward: require large signal-to-noise ratios and/or make the bandwidth-to-loop carrier frequency as small as possible (high Q). Substituting some pessimistic numbers into this equation yields some interesting insight into the importance of each of these factors. Assume a 100 cps bandwidth loop operating at 500 kc with a 6 db ($\rho = 2$) signal-to-noise ratio.

$$\frac{\epsilon}{f_o} = \frac{4 \times 10^{-8}}{6} \times .135 \approx 10^{-9} \quad (1-3)$$

From this favorable result, it might be concluded that, if the loop can be brought above threshold and kept in lock, a counting of the zero crossings will yield an accurate result. The primary assumption was that it was the long term average frequency desired. In doppler counting, since the frequency is shifting with time, data must be collected at short intervals. With the assumption thus weakened, the number given before is somewhat better than what should be expected. The conclusion, however, remains: threshold considerations should dictate receiver design.

1.4 THE THREE CAUSES OF PHASE ERROR

In a doppler loop, the disturbances which may reduce threshold and cause loss of lock may be divided into three categories: (1) noise, (2) signal drift, and (3) equipment instability. Phase lock may be lost for one of the three reasons mentioned, but is almost always a summation of these effects.

1.4.1 Signal Drift

In a receiver designed primarily for the detection and tracking of a pure carrier as it slews in frequency, a type of loop must be chosen that allows a significant amount of tracking range without excessive phase error. The simple low-pass filter that is often used in phase-locked loops for FM detection will not do. For instance, if the block labeled $G(s)$ in the diagrams is something simple, e.g., a straight wire, the error out of the non-linear device is applied directly to the VCO. Since the error is limited by the non-linearity of the phase detector to an output of unity ($\sin \frac{\pi}{2} = 1$), the maximum signal that the VCO can see is unity. When this maximum occurs, the VCO will integrate its relative phase output by K_v rad/sec or $\frac{K_v}{2\pi}$ cps. This, then, is the peak frequency shift that any phase error can command. If the input carrier were to drift $\frac{K_v}{2\pi}$ cps (from the VCO center frequency), the loop would be on the verge of losing lock on that account alone.

By increasing the gain from unity to an arbitrary value, K_g , the loop could track $\frac{K_g K_v}{2\pi}$ cps. However, the bandwidth (signal and noise) would also increase and make a more serious problem. One may overcome this interrelation of tracking width and dynamic bandwidth by specifying $G(s)$ to be an ideal integrator:

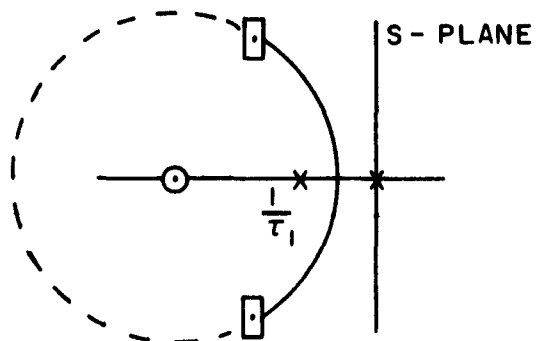
$$G(s) = \frac{K_g}{s} \quad (1-4)$$

As a long-term phase error develops, the integrator output can increase without a proportionate increase in phase error and when it succeeds in matching the phase, the integrator can hold its value with no phase error. There is one difficulty. In order to stabilize the loop, $G(s)$ must include a zero (see Fig. 1-2a and 1-2b). This condition does not interfere with the integrating action, but it does add to the complexity of the system and affects the noise bandwidth as seen in the next section.

With an integrating $G(s)$, the phase error may be brought to zero for any fixed frequency shift. A steady-state phase error will exist, however, for a constant rate of drift. It is

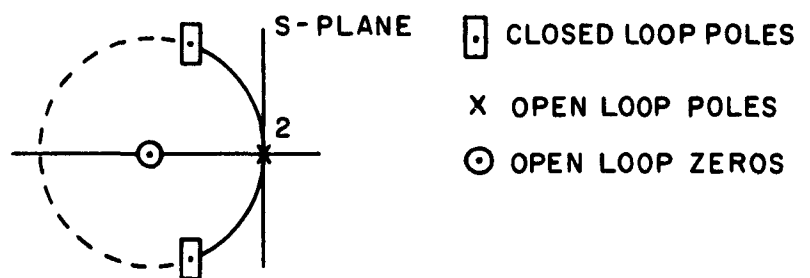
$$\theta_{e_{ss}} = \frac{\text{drift rate (cps/sec)} \times 2\pi}{K_g K_v} \quad (1-5)$$

It would seem from the above equation that one could achieve any amount of signal drift and that drift rate was the only limitation for a given loop gain. This would be correct except that a physical limitation requires that we modify the model used for $G(s)$. The limitation occurs because of leakage normally encountered in electronic integrators. Leakage results in imperfect integration and causes the pole to move from the origin to the left-half S-plane. Future discussion will be limited to this type of filter.



DWG A12450

Fig. 1-2a Non-Perfect Integrator Loop Dynamics



DWG A12451

Fig. 1-2b Dynamics of Loop Stabilized with an Ideal Integrator

In this type of loop, some phase error is required to hold the VCO at any frequency other than the design center. The phase error available for the purpose of slewing the loop is reduced by this amount. As shown in Fig. 1-3a, the maximum allowable drift rate at center frequency (i.e., the frequency where no phase error is required) is $K_V K_g / 2\pi$. To either side, this value varies depending on the amount of phase error due to frequency offset. As the loop tracks in a particular direction, the maximum available rate in that direction decreases. The poorer the integrator, the more steep is the slope. Fortunately in doppler tracking applications, maximum tracking rates are required near the design center as the satellite passes the relative zenith.

One could set up a criterion for the required loop gain as a function of time with respect to the time of the satellite passes overhead. Also involved in the exact calculation would be the altitude of the satellite, the frequency of transmission, the peak elevation angle, and the amount of phase error allowable to this source of error. Without going into the detail of the actual calculation, it may be readily seen by referring to Figs. 1-3a and 1-3b, that the loop gain would be small at the beginning and end of the pass and would be larger at the time of relative zenith.

We shall return to this discussion and show a means for automatically determining the best bandwidth after exploring the problems introduced by noise and equipment instabilities.

1.4.2 Noise

For the loop which is already in lock, the noise may be assumed to be applied after the phase detector as shown in Fig. 1-1. The final effect of the noise in causing loss of lock may be regarded to exist only in the phase jitter of the VCO about the mean phase. Figs. 1-4a and 1-4b show the loop as it appears to noise. The output variable of interest is variations on θ_2 (VCO phase jitter).

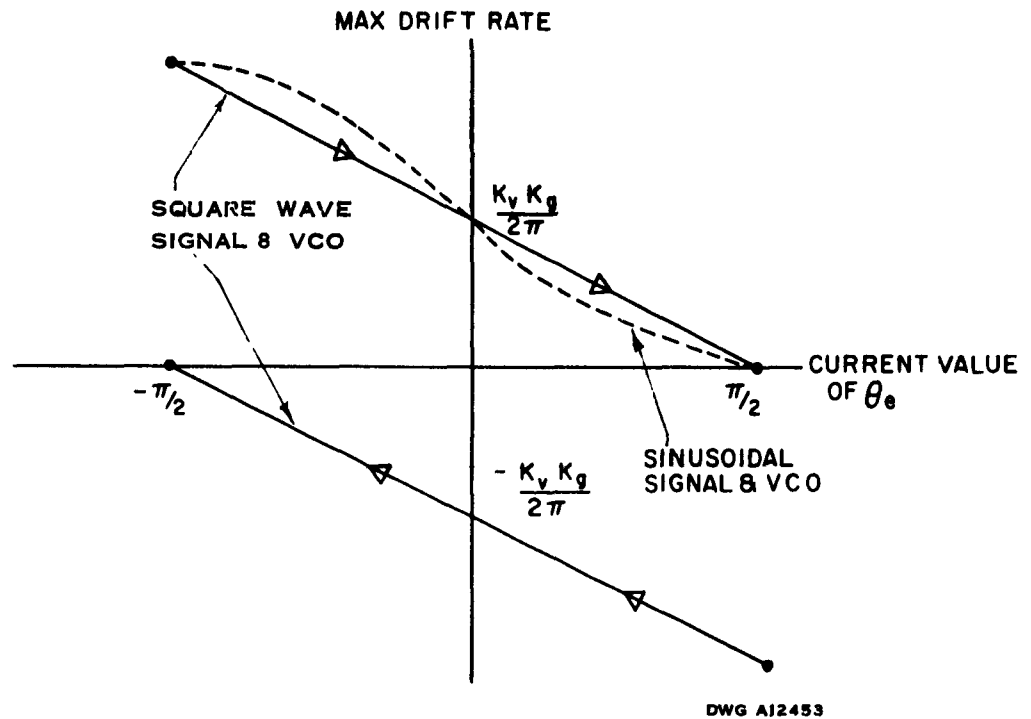


Fig. 1-3a Maximum Drift Ratio for the Non-Perfect Integrating Loop

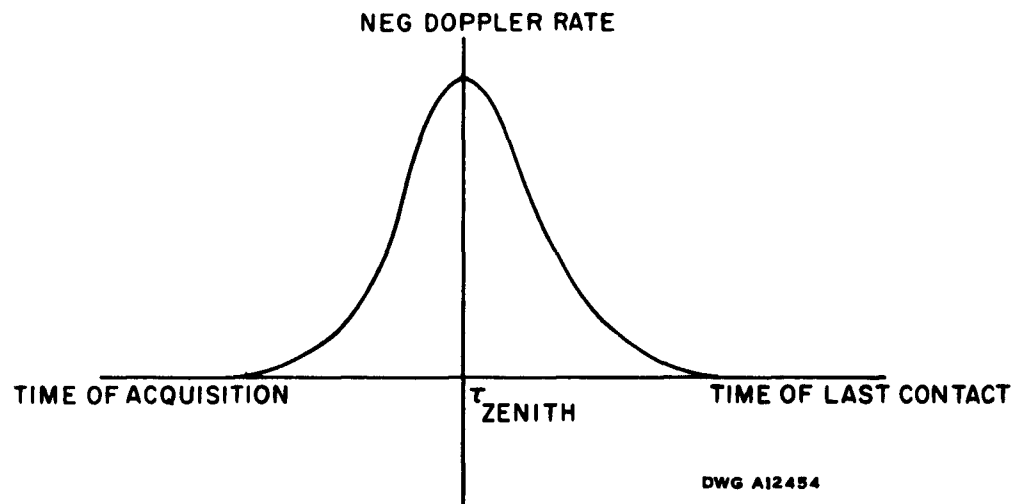


Fig. 1-3b Typical Shape of a Satellite Doppler Rate Curve

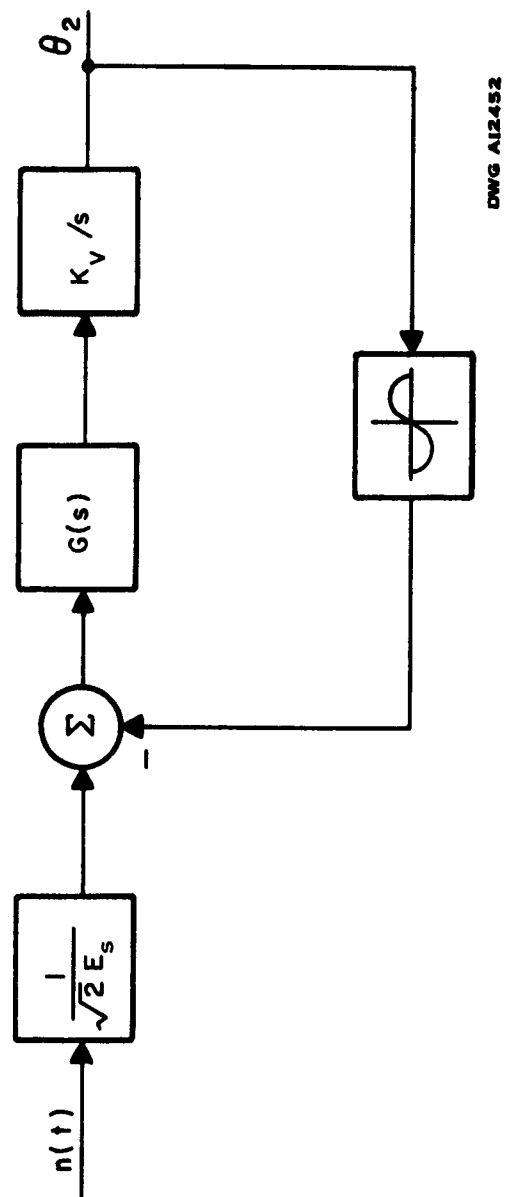


Fig. 1-4a Equivalent Loop for Noise Input Only

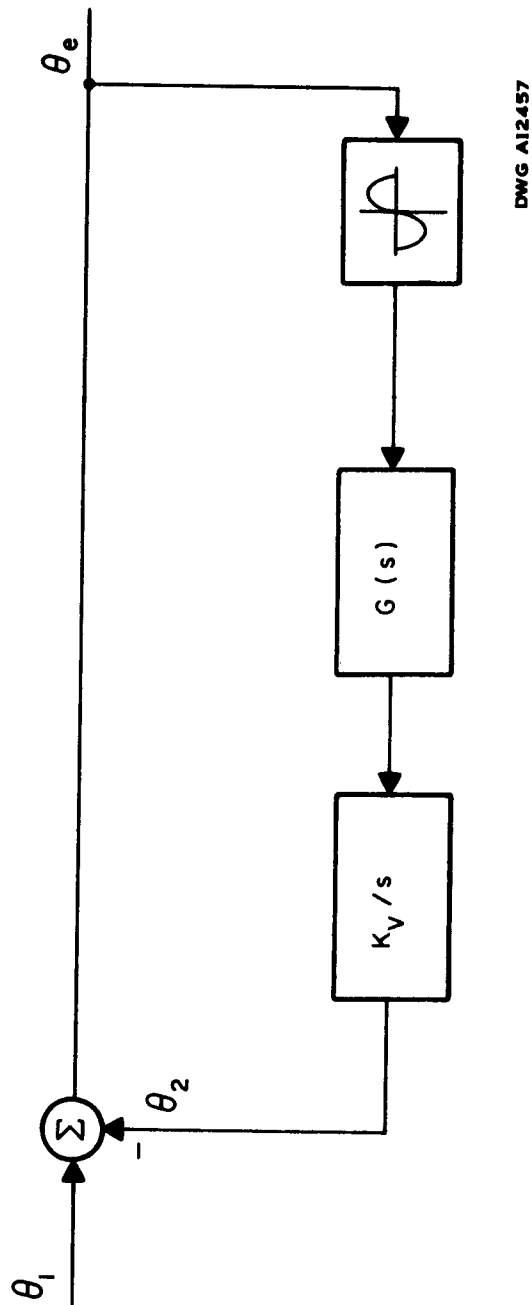


Fig. 1-4b Signal Loop where Phase Error is the Output Variable

The filter which has emerged as desirable has the transfer function:

$$G(s) = k_g \frac{T_2 s + 1}{T_1 s + 1} \quad (1-6)$$

As may be found from the loop configuration shown in Figs. 1-4a and 1-4b and the above function, the overall loop transfer function to noise is

$$\frac{O_2(s)}{N(s)} = \frac{1}{\sqrt{2} E_s} \frac{\frac{K_g K_v T_2}{T_1} s + \frac{K_g K_v}{T_1}}{s^2 + \frac{K_g K_v T_2 + 1}{T_1} s + \frac{K_g K_v}{T_1}} \quad (1-7)$$

and if $K_g K_v T_2 \gg 1$ is similar to

$$K \frac{2\zeta\omega_n + \omega_n^2}{s^2 + 2\zeta\omega_n s + \omega_n^2}$$

where $N(s)$ is a symbolic notation representing a transform of the noise voltage. As a means of comparison, the noise bandwidth is plotted relative to an ideal filter. Making use of tabulated integrals², Fig. 1-5 shows that for this loop the noise bandwidth reaches a minimum for a damping ratio of one-half.

Holding the damping ratio fixed, it may be seen from Equation 1-7 that the noise bandwidth is proportional to the square root of $K_g K_v / T_1$.

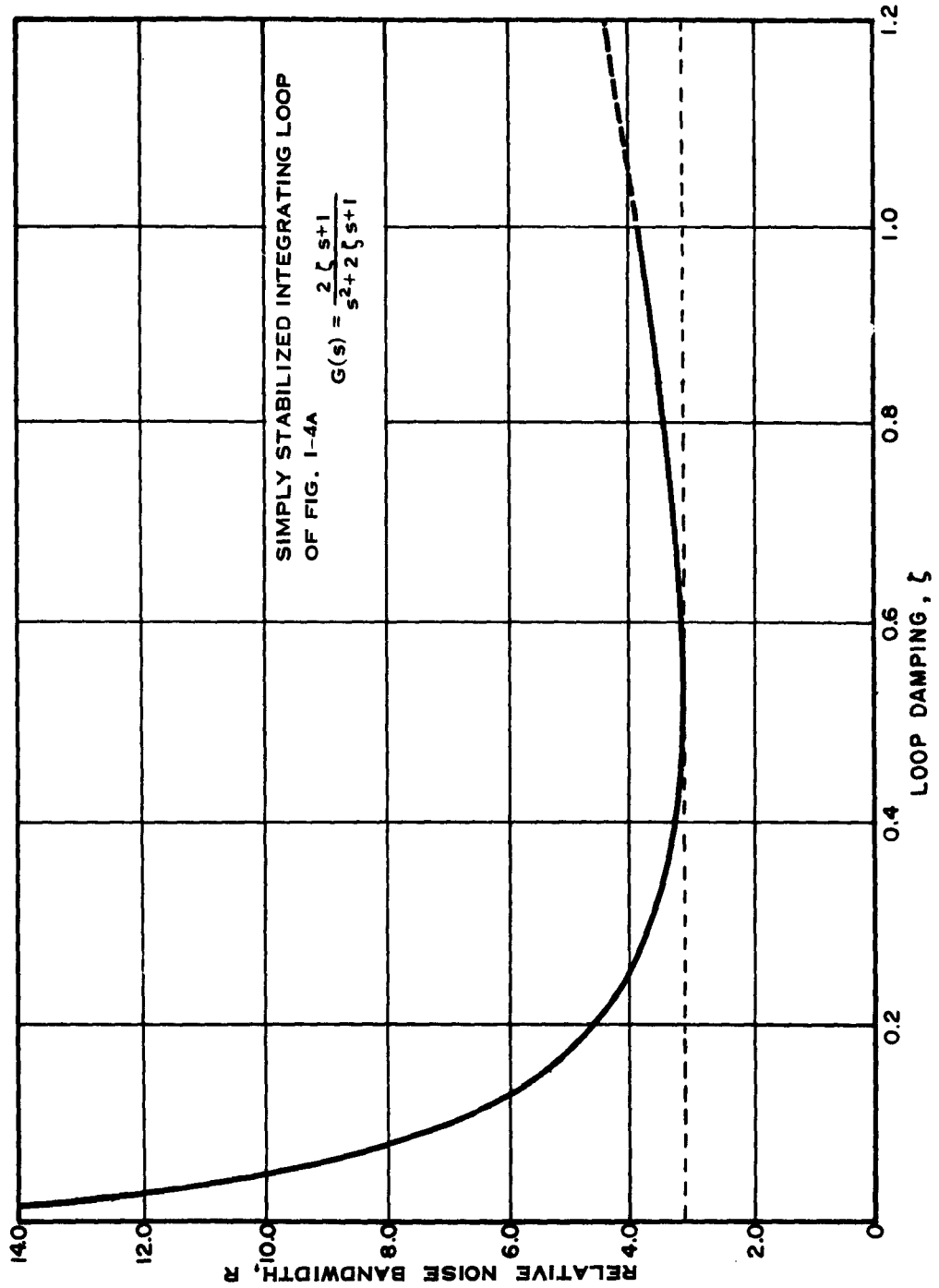


Fig. 1-5 Relative Noise Bandwidth for an Integrating Filter Type of Phase-Locked Loop of Fig. 1-4a

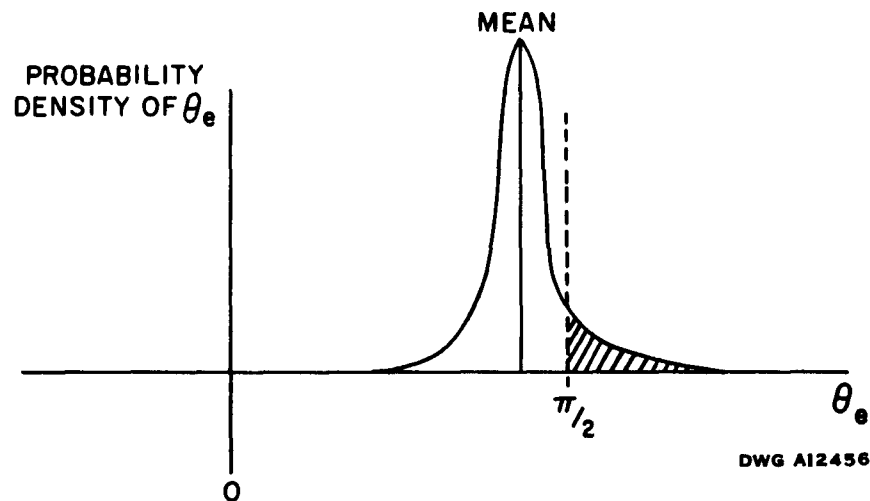
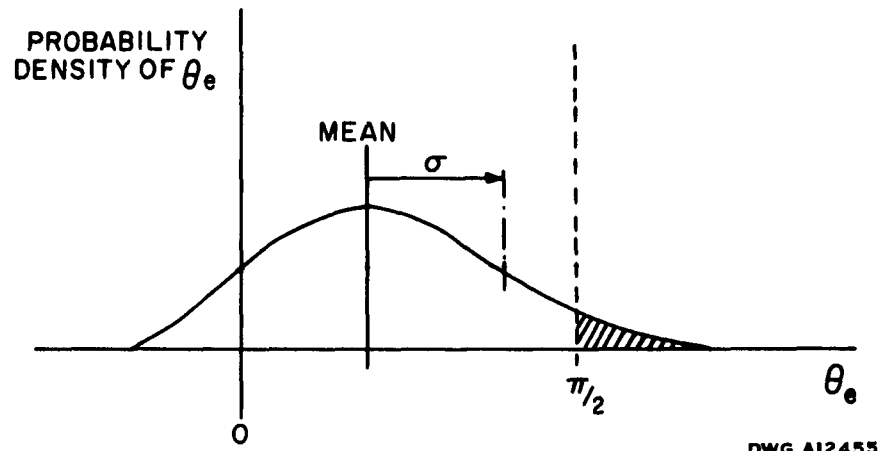
1.4.3 Equipment Instabilities

The prime source of this type of error occurs in the various oscillators used in generating the original carrier, the beating and mixing in the receiver and the variable frequency oscillator used in the phase locked loop. In these, shot noise causes short term phase variations while lumped components such as inductors, capacitors, and quartz crystals change the mean frequency due to temperature and mechanical shock.

The most troublesome source of equipment instability in narrow-band doppler tracking loops is the receiver VCO. The very factors which allow the intentional variation of the oscillator's frequency result in a greater susceptibility to short term phase jitter. This instability is most often the factor which limits how narrow a loop bandwidth may be achieved. This effect will not be considered in the analysis that follows except as limiting the narrowness of the loop bandwidth.

1.5 THE OPTIMUM DESIGN

In designing for the lowest threshold, the bandwidth must be chosen so as to minimize the probability that the instantaneous phase error exceeds $\pi/2$. The phase error is a random variable whose mean is due to the phase offset needed to cause the VCO to follow the carrier with doppler and whose variance is equal to the noise power in θ_2 ; the VCO phase jitter. The mean for a particular set of conditions will increase as the bandwidth is reduced. At the same time variance will decrease. It is apparent, then, that the bandwidth is the variable to optimize. Figs. 1-6a and 1-6b compare two widely different conditions which result in similar thresholds as noted by the similar shaded areas.



Figs. 1-6a (top), 1-6b Two examples Resulting in a Similar Threshold Value

If a designer were given a particular satellite pass to use as a design standard, it would be possible for him to compute and pre-program the optimum bandwidths. However, a much more general solution to the problem exists in a self-adaptive receiver.

The adaptive receiver could make measurements of the average phase error (mean of the random variable) and the phase noise level at this output of the VCO (the variance of the distribution). From this it could trade-off one voltage against the other to determine the required action to increase or decrease the loop bandwidth.

If however, the receiver is able to change loop bandwidth and still retain the same relative noise bandwidth (i.e., retain a similar pole-zero configuration) a simpler solution is described in Appendix A. It is shown there that the optimum bandwidth is proportional to the square root of the doppler drift rate without respect to signal power or noise power density. Specifically, if a compromise of the two solutions given in Appendix A is taken;

$$\omega_n = \sqrt{\frac{4}{L}} |\dot{\omega}|$$

A voltage proportional to ω is available at the input to the VCO. The bandwidth command can be formed by differentiating this voltage and passing it through a non-linear device to perform the absolute value and square root operation.

The relationship for an alternate and more easily implemented method is found by manipulating the above equation and the expressions for loop bandwidth. The final result is that absolute value of the phase error should be maintained as close as possible to $\theta_e = L/4$ and, since L is usually considered to be $\pi/2$, $\theta_e = \pi/8$ or 22.5 degrees.

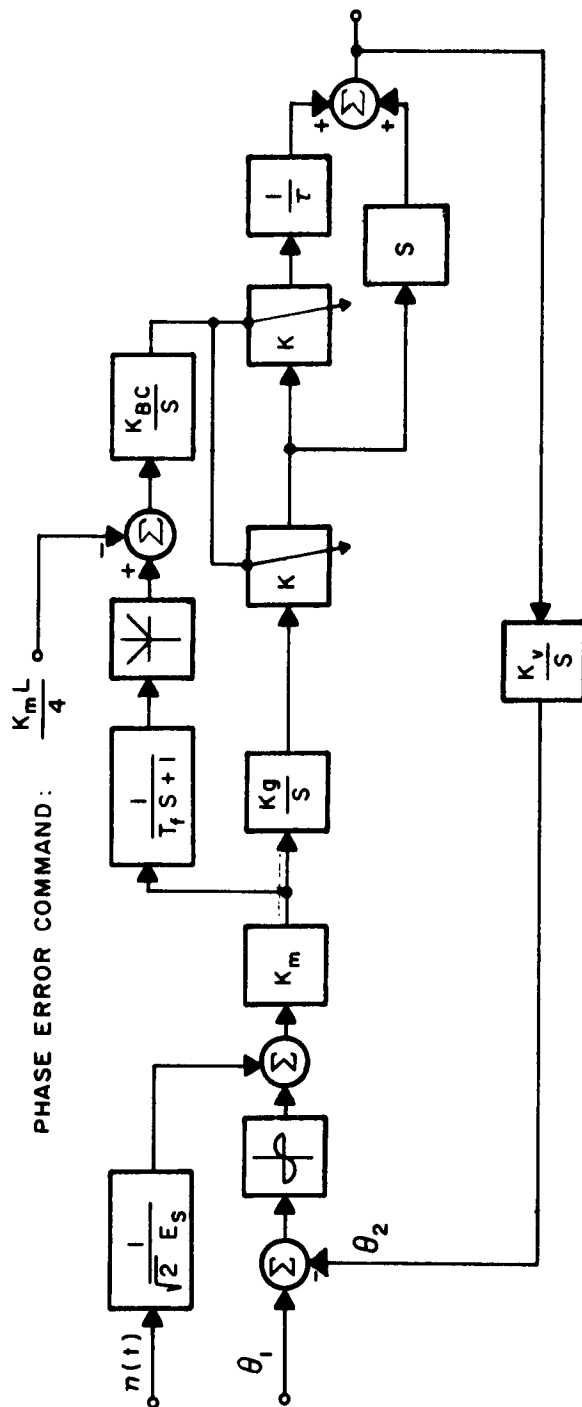
The implementation of this second method may be accomplished as diagrammed in Fig. 1-7. A voltage is taken from the output of the phase detector and filtered to remove most of the noise. The filtered signal is summed in absolute value with a negative voltage equivalent to the required phase offset. If the criteria of $\theta_e = L/4$ is met, the output of the summer is zero. If an error exists, the integrator which follows will integrate in a direction to correct the bandwidth. The absence of a doppler signal will decrease the bandwidth to the narrowest allowed.

A review of the assumptions is in order so that this simple and easy-to-implement rule may not be misapplied. The assumptions are:

- a. The carrier being tracked has no modulation
- b. The long term phase error offset is due to a drifting signal (doppler)
- c. A change in the loop bandwidth causes all pole and zero locations to be scaled proportionally
- d. The criterion for goodness is the maximization of the probability of the instantaneous phase error not exceeding some limit ($\pm \pi/2$)

1.6 VARIABLE BANDWIDTH LOOP DESIGN

It is desired to design a phase-locked loop with controllable closed loop bandwidth. Because the loop must have a large tracking range to track a carrier with doppler, the loop filter will have an integrator (or very long time constant). Type II loops (one active integrator and a VCO) are inherently unstable without the phase lead contributed by a zero in the open loop transfer function. This leads us to a general formulation of the servo control problem.



DWJ AI2461

Fig. 1-7 The Adaptive Bandwidth Detector

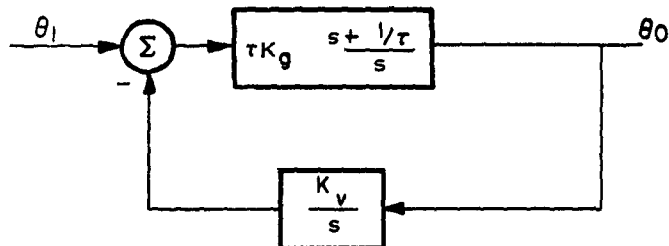


Fig. 1-8 Simple Block Diagram

The closed loop transfer function is $\frac{\theta_o(s)}{\theta_1(s)} = \frac{\tau K_g s (s + 1/\tau)}{s^2 + K_v K_g \tau s + K_v K_g}$ (1-8)

To see how bandwidth, ω_n , and damping ratio, ζ , enter into this expression, compare it with the generalized form

$$\frac{\theta_o(s)}{\theta_1(s)} = K \frac{s (s + \zeta \omega_n)}{s^2 + 2\zeta \omega_n s + \omega_n^2} \quad (1-9)$$

The term ω_n is incorporated in the numerator to allow the open loop zero to move as the required closed loop bandwidth move. In this manner the change of bandwidth amounts to a rescaling of the s -Plane and the root locus. If we now attempt to incorporate a variable gain, K , into each term in the first equation where ω_n occurs in the second, the following form results:

$$\frac{\theta_o(s)}{\theta_1(s)} = \frac{K_g s (s + K/\tau)}{s^2 + K_v K_g \tau s + K_v K_g K^2} \quad (1-10)$$

A linear change in K will cause a linear change in the closed loop bandwidth while retaining the same relative bandwidth (no change in ζ or the loop configuration). The mechanization of this is shown in Fig. 1-7. As the value of K is varied from 0 to 1, the loop bandwidth will go from 0 to the designed value (dependent on K_g , K_v , and τ). Equipment instabilities will make it undesirable for the bandwidth to become zero so in the actual design, steps will be taken to limit the values of K from ϵ to 1.

WDL-TR1948

SECTION 2
RECEIVER DESCRIPTION

SECTION 2

RECEIVER DESCRIPTION

2.1 GENERAL

This section describes the hardware developed for the experimental adaptive detector. The detector incorporates a basic phase-locked loop, automatic search, and adaptive bandwidth circuitry. The bandwidth is metered as is the analog output. Provision is made to monitor the VCO frequency and to disable the sweep and adaptive circuits to allow manual operation.

The following problems had to be solved during development of the present circuitry:

- a. Design of a loop with a known and variable transfer function incorporating an active integrator
- b. A method by which the gain, and therefore the bandwidth of the loop, may be varied by a control voltage
- c. A means of deriving the control voltage by sampling the phase error and the noise present
- d. A search and lock-on circuit
- e. A stabilized VCO necessary for very narrow loops.

The first three items above have been completed and the loop has been closed and the bandwidth control voltage varied manually. Phase jitter and instability at narrow bandwidths led to some work on (e), without significant success. Work is in progress on (c) and the circuitry involved will be covered in a supplemental report.

2.2 ADAPTIVE DOPPLER TRACKING DETECTOR

2.2.1 Operation with no Signal

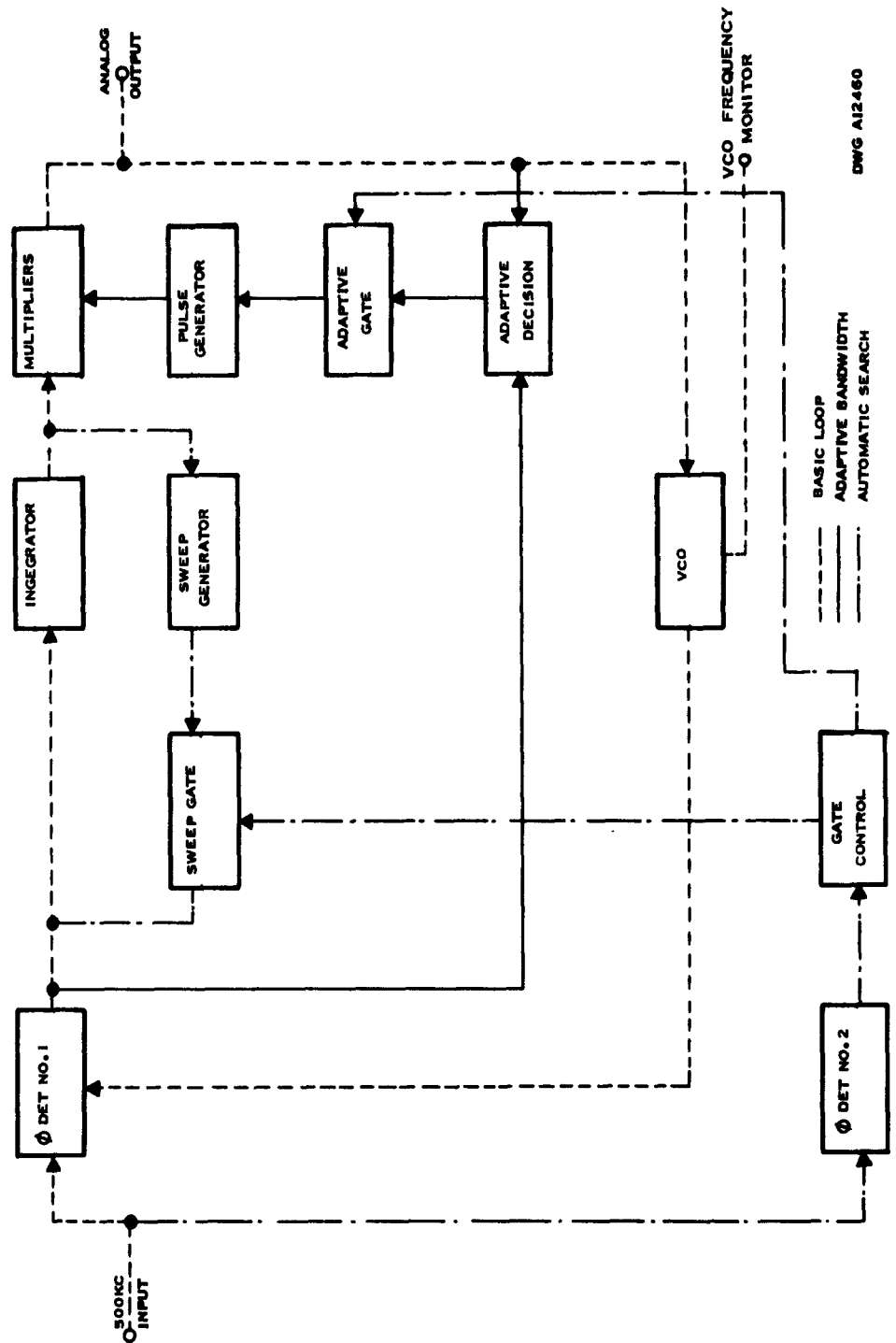
Figure 2-1 shows a block diagram of the detector. In the absence of a signal, the gate control output holds the sweep gate closed and applies a reference voltage through the adaptive gate to the pulse generator which represents minimum bandwidth. The sweep generator applies a square wave at the integrator input resulting in a triangular voltage being applied to the VCO. Therefore the VCO frequency is swept back and forth several kc either side of center frequency. The output of the phase detectors at this time is zero.

2.2.2 Operation with Signal

When a signal appears at a frequency within the sweep limits of the VCO, the VCO frequency will at some time be the same as that of the signal. At this time, Phase Detector 2 produces an output which causes the gate control outputs to reverse the initial condition of the sweep and adaptive gates. The output of Phase Detector 1 now has control of the VCO via the integrator and multipliers and the condition of lock is achieved. Coincidentally, control of the pulse-width is switched from the reference voltage to the output of the adaptive decision. Now, if the phase error and noise present are such that the loop is too narrow, the adaptive decision will increase the multiplier's output until optimum bandwidth is reached. Any further change in signal and/or noise characteristics will result in a bandwidth change.

2.2.3 Phase Detector 1 (Fig. 2-2)

The incoming signal is first limited to remove amplitude variations and is then applied to a diode gate. The gate is opened and closed by the balanced output of a cathode coupled phase inverter that is driven by the VCO. The output of the gate is zero when a 90° phase difference exists between the signal and VCO. This is the condition when the loop is in lock and if the signal frequency changes, the error voltage developed moves the VCO frequency in a direction to reduce the error to zero. In this manner, the VCO tracks the incoming signal.



DWG A12460

Fig. 2-1 Block Diagram of the Detector

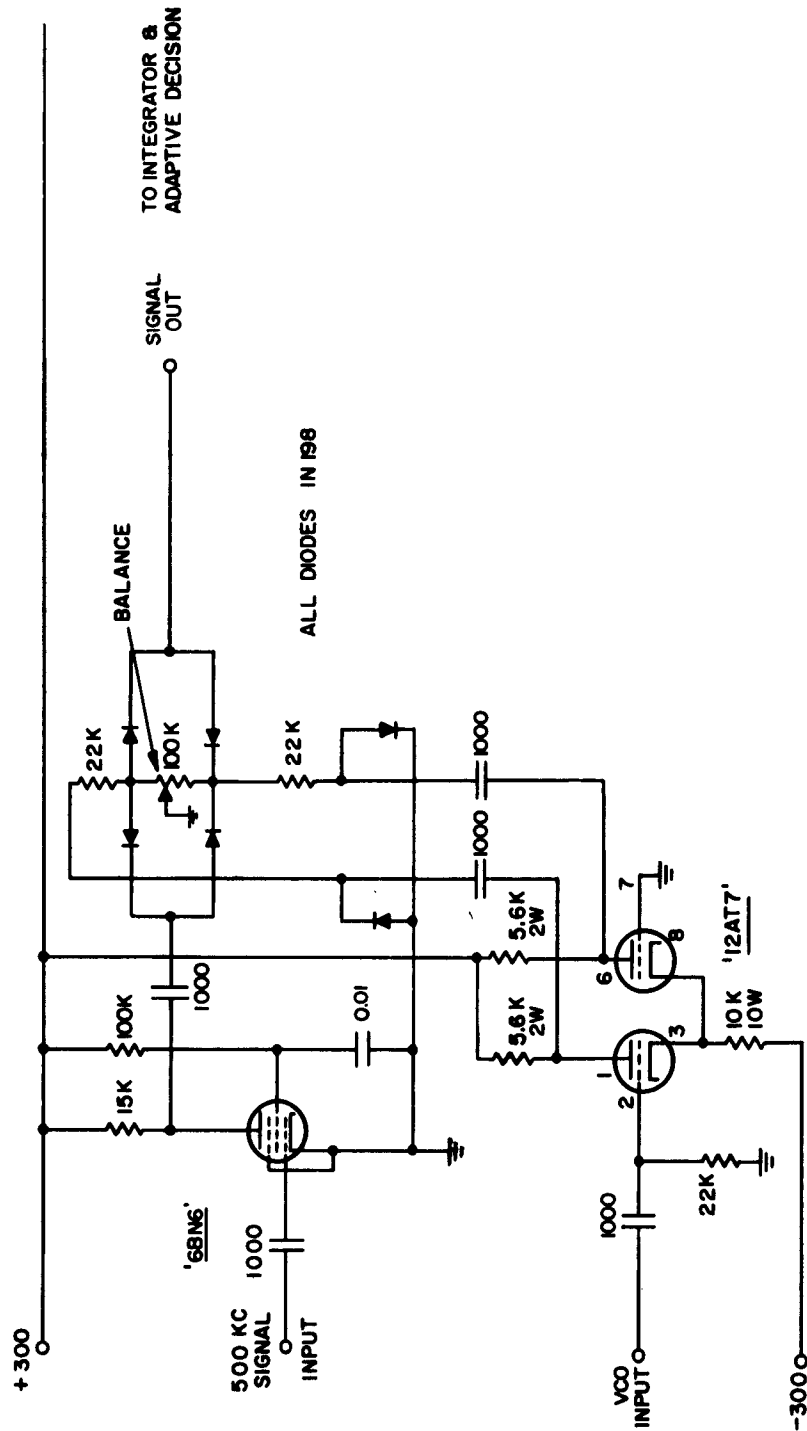


Fig. 2-2 Phase Detector

2.2.4 Integrator (Fig. 2-3)

A stabilized Philbrick operational amplifier with capacitive feedback forms an integrator with a threefold purpose. It filters the phase detector output, allows wide tracking range, and produces the triangular sweep voltage.

2.2.5 Multipliers (Fig. 2-4)

The output of the integrator is first limited to protect the switching transistors, and then applied to the first multiplier. The multiplier is a transistor switch that, when closed, shorts any signal to ground. The time closed is dependent upon the signal present at the base, which is (in this case) a 50-kc pulse with a duty cycle that can be varied from 0 to 1. Since zero output is never desired, a resistor by-passes the multiplier and its value will set minimum bandwidth. The output is filtered to remove the 50-kc component and is applied to another identical multiplier. If the input voltage is 1 volt and the pulse duty cycle is 0.5, the first multiplier output is 0.5 volt and that of the second 0.25 volt.

Shown also in Fig. 2-4 is an amplifier that combines the multiplier outputs to form a lead network. This amplifier also provides a convenient place to off-set the VCO control voltage. This off-set controls the VCO center frequency and is a front panel control.

2.2.6 Voltage Controlled Oscillator (Fig. 2-5)

The VCO is a plate-to-grid coupled multivibrator with the grid resistors returned to the plate of a control tube. The frequency of the oscillator varies in response to any change in voltage at the grid of the control tube. A cathode follower output is provided to recover the carrier frequency and a limited output is used to drive the phase detectors.

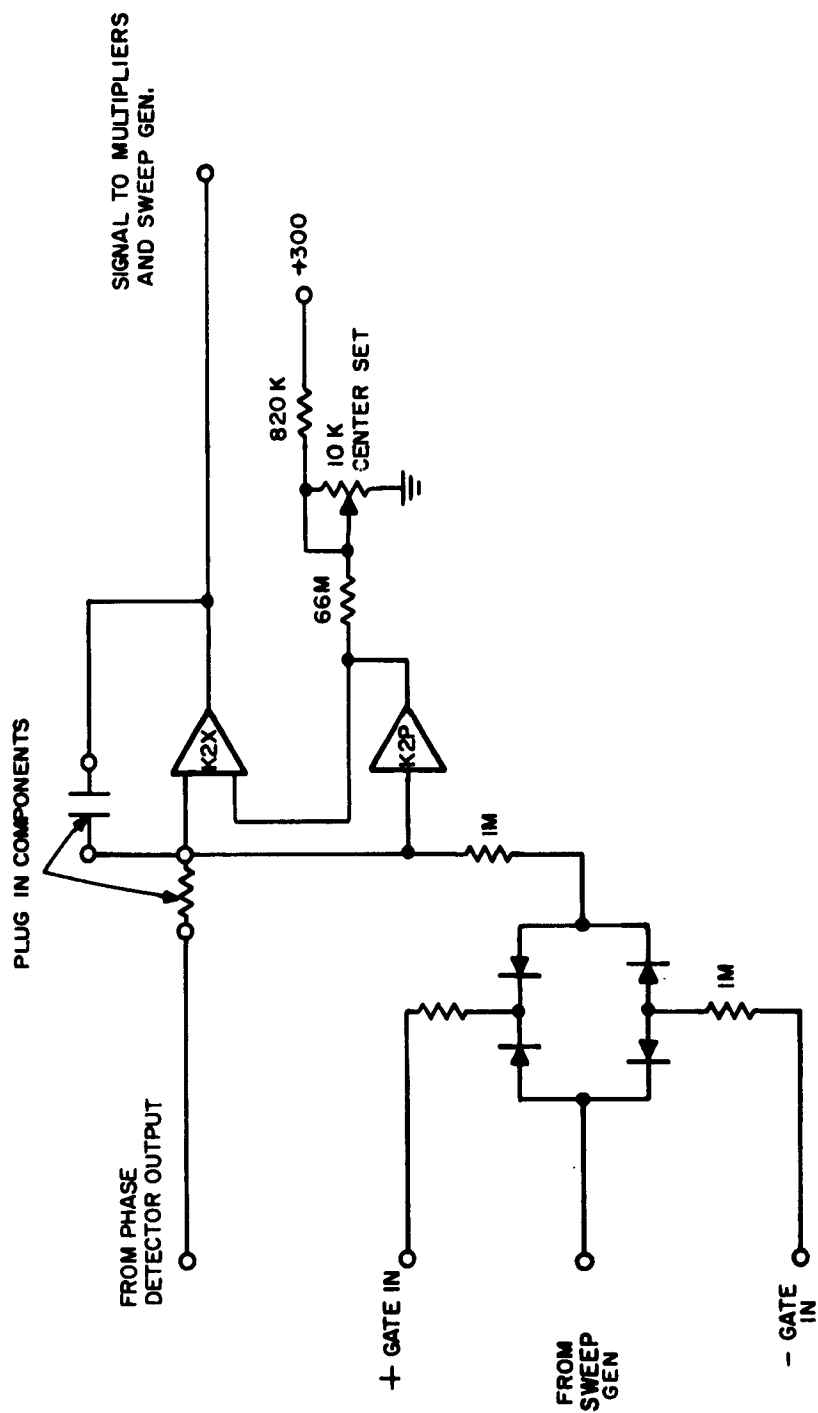
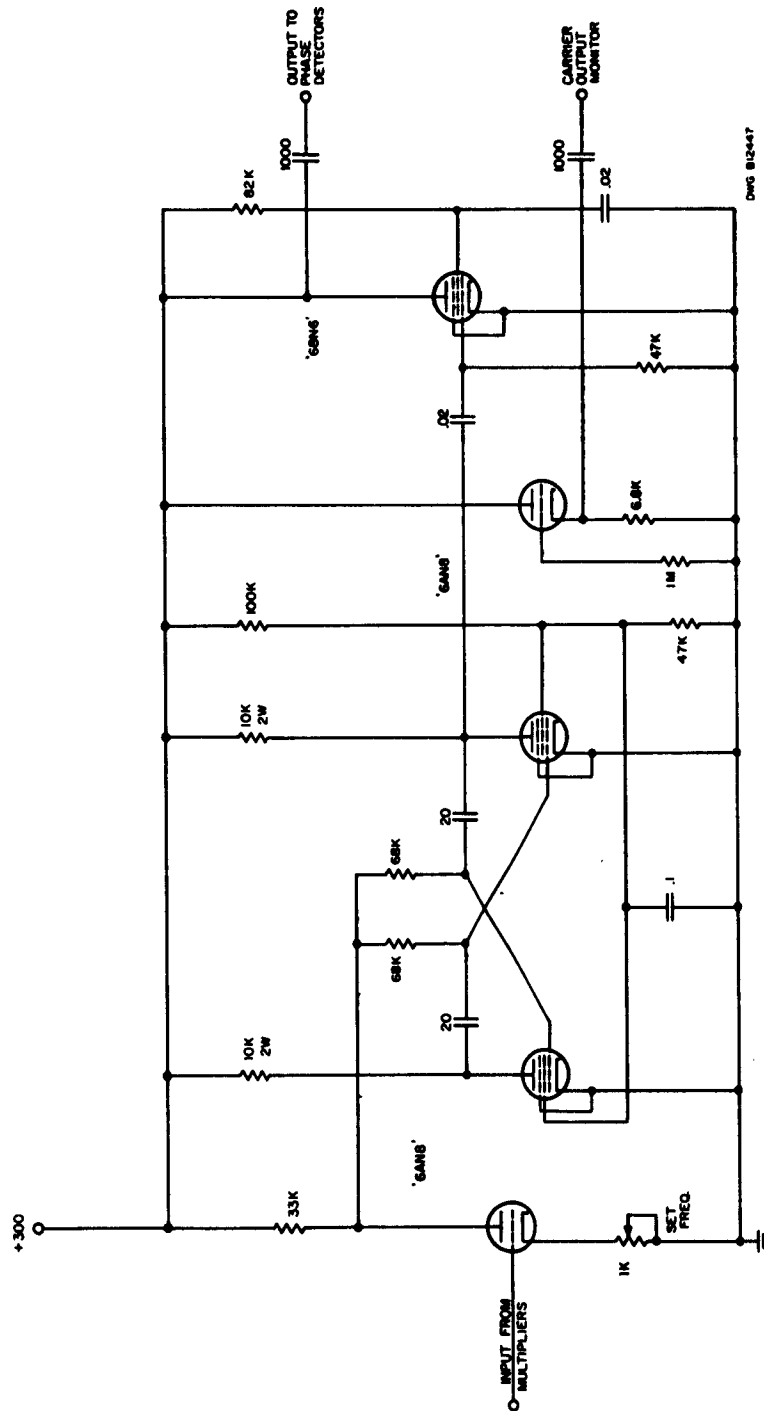


Fig. 2-3 Integrator



Fig. 2-4 Multipliers



DWG 812447

Fig. 2-5 Voltage Controlled Oscillator

2.2.7 Phase Detector 2 (Fig. 2-6)

This phase detector is identical to Phase Detector 1. However, the signal is first shifted 90° by a low Q resonant circuit. This arrangement forms an envelope detector and when the loop is in lock, the signal and VCO are 180° out of phase causing a negative output voltage. This voltage operates the gate control.

2.2.8 Gate Control (Fig. 2-7)

Three Philbrick operational amplifiers in series comprise the gate control circuit. Prior to lock, the gate polarities are reversed from those shown on the schematic. The output of the first amplifier is negative so the inlock indicator lamp is out. When Phase Detector 2 indicates lock by a negative output voltage, each amplifier output reverses. The indicator lamp lights, the sweep gate opens, and the adaptive decision takes control of the bandwidth.

2.2.9 Variable Pulse Width Generator (Fig. 2-8)

A 50-kc triangular wave is generated by integrating a square wave derived from a multivibrator. This voltage and a variable bias voltage are combined and applied to the input of a Schmidt trigger circuit. The triangular wave triggers the Schmidt and the duty cycle is variable from 0 to 1 by means of the bias voltage.

2.2.10 Sweep Generator (Fig. 2-9)

The sweep generator consists of a threshold device and amplifier in conjunction with the integrator. When the sweep gate is closed, some voltage is applied to the integrator input. The integrator then moves in the direction of this voltage until one of the thresholds is reached; at which time the polarity of the integrator input voltage is reversed. The integrator output reverses until the other threshold is reached and the cycle repeats. Thus, a triangular sweep voltage is produced. Sweep width is adjusted by the threshold setting while sweep rate is controlled by adjusting the amplitude of the square wave applied to the integrator.



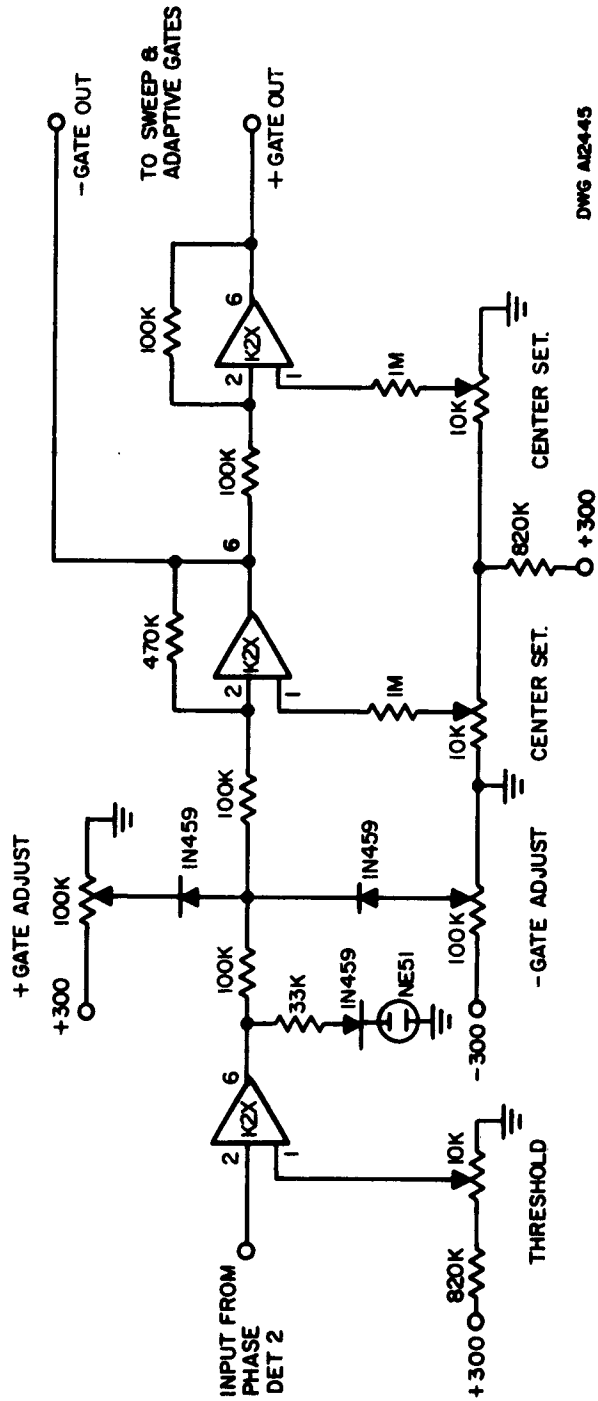
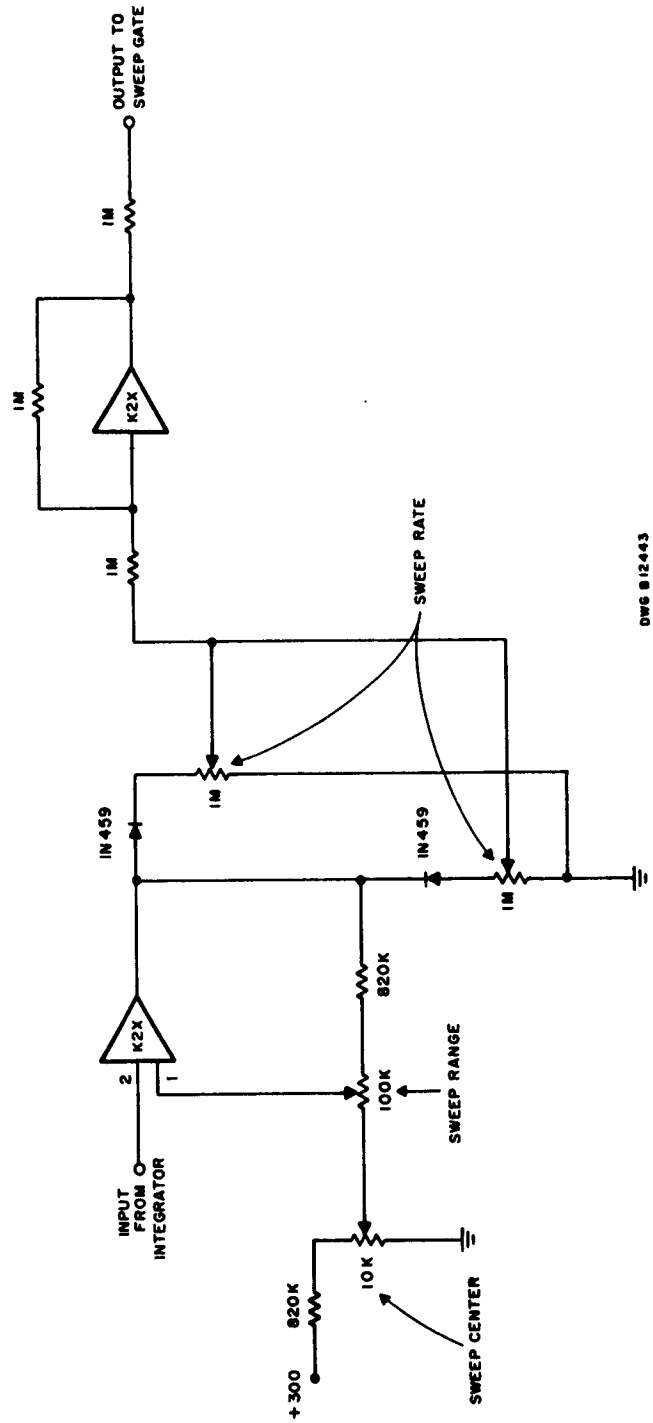


Fig. 2-7 Gate Control



Fig. 2-8 Variable Pulse Width Generator



DWG 812443

Fig. 2-9 Sweep Generator

WDL-TR1948

SECTION 3
OPTIMIZING PHASE-LOCKED LOOP LOCK-ON

SECTION 3

OPTIMIZING PHASE-LOCKED LOOP LOCK-ON

3.1 GENERAL

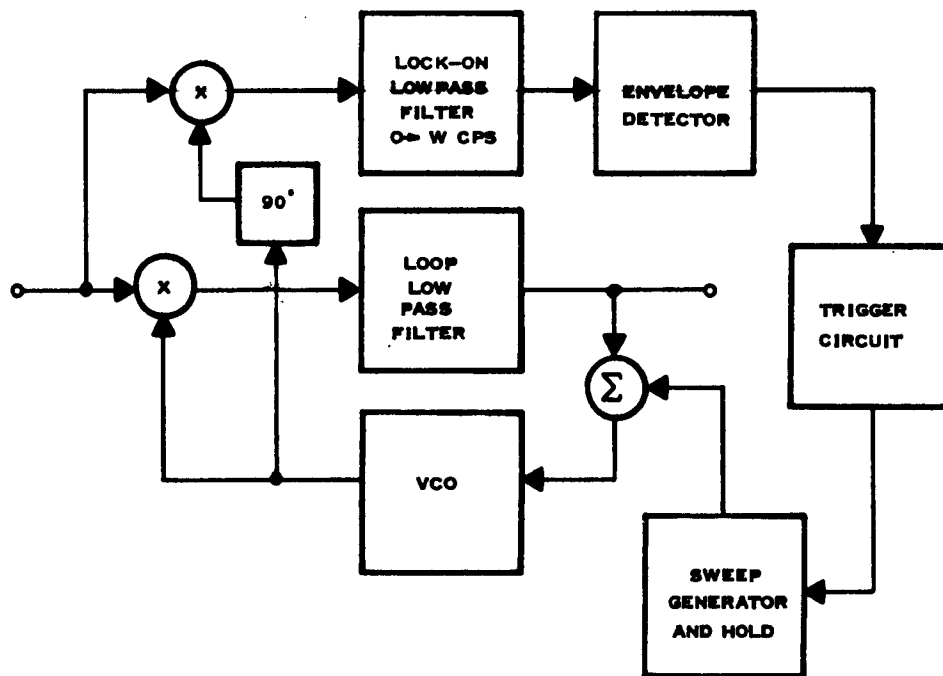
This section contains a general analysis of the usual phase-locked loop lock-on procedure, and illustrates that this is not an optimum method. The system that provides the shortest lock-on time is also described, and formulas and a description of the optimum sweep type acquisition circuit are also contained in this section.

3.2 LOCK-ON PROCEDURE

The lock-on procedure most commonly used is more or less independent of the loop transfer function. Therefore, the characteristics of the loop (other than the pull-in range) will not be considered in the analysis.

When the VCO is near the signal frequency, the resulting beat note is passed through the lock-on low-pass filter, changing the sweep and hold circuit to the hold mode. (See Fig. 3-1). The beat note must remain in the pass-band on the lock-on filter long enough to insure that the output of the envelope detector trips the trigger (assuming instantaneous trigger operation). Even with no signal, there will be an output from the detector due to noise. Thus, the trigger circuit will contain a threshold, which will be set high enough to insure that there will be only a small likelihood that the trigger will be operated by noise alone.

The relationship between this lock-on circuit and the optimum lock-on procedure can be shown by means of the likelihood ratio. In making a decision between the presence or absence of a signal, it is best (in a statistical sense) to use a likelihood ratio test. The likelihood ratio is the ratio of two conditional probability densities,



DWG A12442

Fig. 3-1 Block Diagram of a Typical Loop Sweep and Lock-On Circuit

$$L[x(t)] = \frac{P[x(t)|\omega_1]}{P[x(t)|\omega_0]} \quad (3-1)$$

The voltage $x(t)$ is a waveform that runs from $t = 0$ to $t = T$. The signal may or may not be contained in $x(t)$, depending on which hypothesis, ω_0 or ω_1 , is actually true, e.g.,

$$x(t) = n(t) \quad \text{if } \omega_0 \text{ is true}$$

$$x(t) = s(t) + n(t) \quad \text{if } \omega_1 \text{ is true}$$

Where $x(t)$ and $s(t)$ are the noise and signal waveforms. When

$$L[x(t)] > \beta \quad (3-2a)$$

we say a signal is present.

If

$$L[x(t)] < \beta \quad (3-2b)$$

we say that no signal is present.

The joint probability of independent noise and signal is

$$\begin{aligned} P[n(t), s(t)] &= P_n[n(t)] P_s[s(t)] \\ &= P_n[x(t) - s(t)] P_s[s(t)] \\ &= P[x(t)/s(t)] P_s[s(t)] \\ &= P[x(t), s(t)] \end{aligned} \quad (3-3)$$

Averaging over all $s(t)$ gives the marginal distribution for $x(t)$ or

$$P [x(t)/\omega_1] = \int_{s(t)} P_n [x(t) - s(t)] P_s [s(t)] ds(t) \quad (3-4)$$

P_n and P_s are the noise and signal distributions. Also

$$P [x(t)/\omega_0] = P_n [x(t)]$$

Then

$$L [x(t)] = \int_{s(t)} \frac{P_n [x(t) - s(t)] P_s [s(t)] ds(t)}{P_n [x(t)]} \quad (3-5)$$

If $x(t)$ is a band limited function of bandwidth W (see Fig. 3-2 extending from 0 to T , one can expand $x(t)$ by the well known sampling theorem into the series,

$$x(t) = \sum_{i=0}^{2TW} x_i \psi_i \quad (3-6)$$

$$x_i = x \left[i \frac{1}{2W} \right] \quad (3-7)$$

$$\psi_i = \frac{\sin \pi 2TW \left[\frac{t}{T} - \frac{i}{2TW} \right]}{2TW \sin \left[\frac{t}{T} - \frac{i}{2TW} \right]} \quad (3-8)$$

where $x(t)$ is assumed to be zero outside the interval $[0, T]$ and sampling is at a rate of $2W$ samples per second.

Since $x(t)$ is completely determined by the sample values, x_i , we can write P_n as a joint distribution

$$P_n [x(t)] = P_n [x_0, x_1, \dots, x_{2TW}] \quad (3-9)$$

We will assume that P_n is Gaussian. Then the joint distribution is

$$P_n [x(t)] = \frac{1}{\sqrt{(2\pi)^n K}} e^{-\frac{1}{2} X_t K^{-1} X} \quad (3-10)$$

Where X is the vector.

$$X = \begin{bmatrix} X_0 \\ X_1 \\ \vdots \\ \vdots \\ \vdots \\ X_{2TW} \end{bmatrix}$$

and X_t is the transpose. The matrix K is the covariance matrix of the X_i 's when no signal is present, or the noise covariance matrix.

We are hypothesizing a signal that is sinusoidal and random in phase and frequency. The phase is uniform between zero and 2π , and the frequency is uniform between zero and W cps. Then

$$P(\theta) P(\omega) d\theta d\omega = P_s [s(t)] ds(t), \quad (3-11)$$

and equation (3-11) is

$$\begin{aligned} l[x(t)] &= \frac{1}{2\pi} \frac{1}{2\pi W} \int_0^{2\pi} \int_0^{2\pi W} \frac{e^{-\frac{1}{2} (x-\vec{s})_t K^{-1} (x-\vec{s})}}{e^{-\frac{1}{2} x_t K^{-1} x}} d\theta d\omega \\ &= \frac{1}{(2\pi)^2 W} \int_0^{2\pi} \int_0^{2\pi W} e^{-\frac{1}{2} [\vec{s}_t K^{-1} \vec{s} - 2\vec{s}_t K^{-1} x]} d\theta d\omega \quad (3-12) \end{aligned}$$

where

$$s_1 = A \sin \left(\omega \frac{1}{2W} + \theta \right) \quad (3-13a)$$

$$\vec{S} = \begin{bmatrix} s_0 \\ s_1 \\ \vdots \\ s_{2TW} \end{bmatrix} \quad (3-13b)$$

K will now be simplified to the case where there is independence between noise samples. This would be true if the filter from zero to W were sharply cut off.

$$K = NI \quad (3-14a)$$

$$K^{-1} = \frac{1}{N} I \quad (3-14b)$$

where N is the noise power and I is the identity matrix. For $2TW$ sufficiently large, $S_t S$ is very nearly equal to $2TW \frac{A^2}{2}$, where $\frac{A^2}{2}$ is the average signal power. Thus equation (3-12) is

$$E[x(t)] = \frac{e^{-\left(\frac{1}{2W} \frac{A^2}{2N} \right)}}{(2\pi)^2 W} \int_0^{2\pi} \int_0^{2\pi W} e^{\frac{S_t x}{N}} d\theta d\omega \quad (3-15)$$

Evaluation of this integral is extremely tedious and only the form of the answer will be given here. For the detail see the WDL technical report entitled "Digital Filtering." Integration gives

$$E[x(t)] = C_1 \sum_0^{2TW} x_1^2 + C_2 \quad (3-16)$$

where C_1 and C_2 are functions of the signal-to-noise ratio. A low signal-to-noise ratio is assumed. Then we can say that the signal, $s(t)$ is present if

$$\sum_0^{2TW} x_i^2 > \gamma \quad (3-17a)$$

or absent if

$$\sum_0^{2TW} x_i^2 < \gamma \quad (3-17b)$$

The form of the ideal detector is shown in Fig. 3-2.

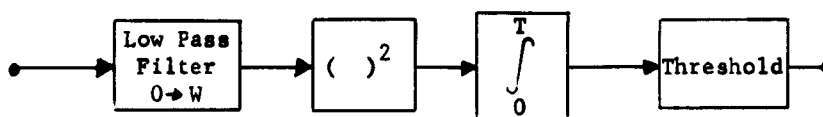


Fig. 3-2 The Ideal Detector

The integrator, integrating from 0 to T is almost equivalent to a low pass filter of bandwidth $\frac{1}{T}$. So a near equivalent to the ideal detector is shown in Fig. 3-3.

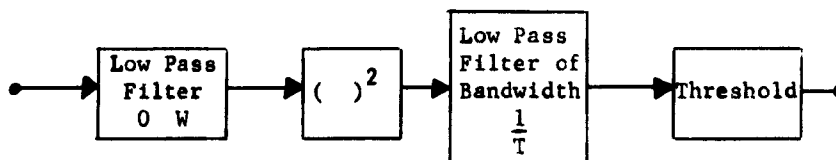


Fig. 3-3 The Near Ideal Detector

The square law device and the low-pass filter form an envelope detector so the form of the detection circuit shown in Fig. 3-1 is correct. The following paragraphs illustrate that a larger T will give a higher probability of acquisition.

As can be seen in Fig. 3-2, there will be a distribution on the output of the integrator assuming that a signal is present, and another assuming no signal is present. So there will be a certain probability that the threshold will be exceeded with no signal and visa versa.

The mean and the variance for the output of a full wave square law device are well-known when the input is Gaussian noise with or without a sinewave signal. For small signals they are:

	<u>Mean</u>	<u>Variance</u>
No signal	N	$2N^2$
Signal plus noise	$\frac{A^2}{2} + N$	$2 [A^2 N + N^2]$

The distribution of a sum of a large number of independent samples of $x(t)$ will be nearly Gaussian (central limit theorem). The variances and mean of a sum of $2WT_0$ identically distributed independent samples are $2WT_0$ times the variance and the mean of one sample. Thus, the difference between the means of the sums (with and without signal) goes up as $2WT_0$, and the two standard deviations go up as $\sqrt{2TW_0}$. If the standard deviations and means of the two distributions (see Fig. 3-4) are normalized by dividing by $[4WT_0 N^2]^{\frac{1}{2}} = \sqrt{2} N^2 \times \sqrt{2WT_0}$, it is seen that the distributions move away from each other faster than the standard distributions increase as T_0 gets large, and the error probabilities decrease.

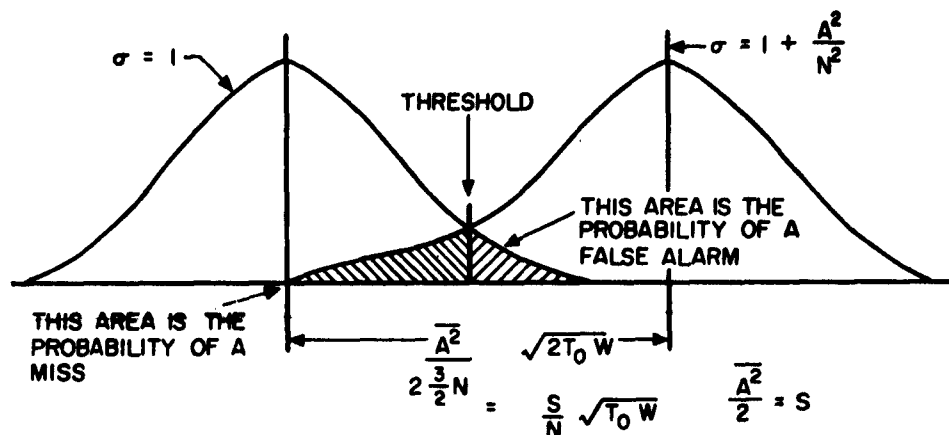


Fig. 3-4 The Error Probabilities for a Signal Channel

If the threshold is set midway between the means, and the distance from the threshold to a mean is k , then

$$T = \frac{4k^2}{\left(\frac{S}{N}\right)^2 W} = \frac{4k^2 W}{\left(\frac{S}{N_0}\right)^2} ; \quad (3-18)$$

where N_0 is the noise spectra density, and k , is a measure of the error probability. For $k = 2$, the probability is 0.03.

To summarize, concerning the optimum detector: when the VCO is swept as in Fig. 3-1 for a given signal-to-noise ratio, there is a maximum pull-in range for the phase-locked loop. The low-pass filter ahead of the envelope detector should be no wider than this pull-in range, because the beat note between the VCO and signal may be anywhere in the filter bandpass. This puts the upper bound on W .

The means and variances given on the preceding pages are true for a signal-to-noise ratio of less than 3 db. It can be shown that decreasing W and thus increasing the signal-to-noise ratio does not lower T . The beat note must remain in the region from zero to W C.P.S. for this time T . If the S/N ratio is greater than 3 db, narrowing the predetection filter will not lower the "dwell" time, but will decrease the sweep rate (i.e., it will increase the average acquisition time). So we have a lower bound on W . If the pull-in range is less than the filter bandwidth which gives a 3 db signal to noise ratio, W should equal this smaller value.

If the signal-to-noise ratio is less than 3 db, decreasing W will not increase the sweep rate, R_s ; since

$$\begin{aligned}
 R_s &= \frac{W}{T} \\
 &= \left[\frac{S}{N_o} \frac{1}{2k} \right]^2 \\
 &= \left[\frac{S}{4N_o} \right]^2
 \end{aligned}
 \tag{3-19}$$

The last line is for a 97 percent probability of acquisition in the first sweep.

The receiver noise figure is defined as

$$F_r = \frac{N_r}{KtBG} \tag{3-20}$$

N_r is the noise out of the receiver, K is Boltzman's constant, t is normally set at 300° absolute, B is the receiver noise bandwidth, and G is the receiver gain. Putting Equation (3-20) into Equation (3-19),

$$R_s = \left[\frac{S_1}{4F_r Kt} \right]^2 \tag{3-21}$$

where S_1 is the signal power at the receiver input terminals.

Substitution of Equation (3-20) into Equation (3-18) gives us the time constant of the filter for the envelope detector.

$$T = \left[\frac{4F_r Kt}{S_i} \right]^2 W \quad (3-22)$$

For high signal-to-noise ratios, the mean and variance of the output of the square law device will approach $\left[\frac{A^2}{2} + 1 \right]$ and $2 \left[\frac{A^4}{16} + A^2 + 1 \right]$ respectively; and, again assuming independence between samples, the mean and standard deviation at the output of the integrator are

$$E_I = 2WT \left[\frac{A^2}{2} + 1 \right] \quad (3-23)$$

$$\sigma_I = \sqrt{2} \sqrt{2WT} A \left[\frac{A^2}{16} + 1 \right]^{\frac{1}{2}} \quad (3-24)$$

Normalizing N to one, and dividing through by $\sqrt{2} \sqrt{2WT}$ gives for the signal case

$$\sigma_s = A \left[\frac{A^2}{16} + 1 \right]^{\frac{1}{2}} \quad (3-25)$$

$$E_s = \sqrt{WT} \left[\frac{A^2}{2} + 1 \right] \quad (3-26)$$

For the no signal case

$$\sigma_n = 1 \quad (3-27)$$

$$E_n = \sqrt{WT} \quad (3-28)$$

So we see that the distance between the means is

$$E_s - E_n = \sqrt{WT} \frac{A^2}{2} \quad (3-29)$$

Again we want

$$k\sigma_s = \frac{1}{2} [E_s - E_n] \quad (3-30)$$

So that

$$T = \frac{k^2 \left[\left(\frac{S}{N} \right)^2 + 4 \right]}{\left(\frac{S}{N} \right)^2 W} \quad (3-31)$$

$$\rightarrow \frac{k^2}{W}$$

for moderate signal-to-noise ratios.

Then

$$R_s = \left(\frac{W}{k} \right)^2 \quad (3-32)$$

This is independent of the signal-to-noise ratio.

One important assumption we made was independence between sample values from the predetection filter taken at a rate of $2W$ samples per second. For large signal-to-noise ratios, this could be a valid assumption if for example the signal was modulated in a random manner. It can be shown that the optimum detector in such cases has the form of Fig. 3-2 without making the small signal approximation.

For a large, purely deterministic signal (such as a sine wave) the correct analysis would be to calculate the transient response at the output of the integrator for the actual predetection filter used when the input is a swept sine wave for example. This calculation will probably involve a numerical convolution and integration on a digital computer. As a rule of thumb, the sweep rate will be approximately as in Equation (3-32). There will be some variance due to the transient response. It is recommended that the transient response be measured on the bench, and then it is quite simple to pick a threshold value and the probability of lock-on for a given sweep rate.

Intuitively, it is obvious that the fastest lock-on is not by use of a sweep generator. A quicker method is to use a number of parallel narrow-band filters as shown in Fig. 3-5. These filters divide the frequency search range into L equal segments; i.e., if the search range is W_0 wide, G_i passes from $\frac{W_0}{L} (i-1)$ to $\frac{W_0}{L} i$ cycles per second. In the acquisition mode the VCO is set at one end of the search range by the voltage E_0 . When an above-threshold indication is obtained in the i th channel, the loop filter is connected to the VCO, and a d-c voltage, E_i , is applied to the VCO to move it to the frequency indicated by the i th channel. The acquisition time is

$$T_L = \frac{4k^2 W}{\left(\frac{S}{N}\right)_0 L} = \left[\frac{2kF_r Kt}{S_i} \right]^2 \frac{W}{L} \quad (3-33)$$

This latter method is approximately $\frac{L}{2}$ times as fast as a sweep acquisition method.

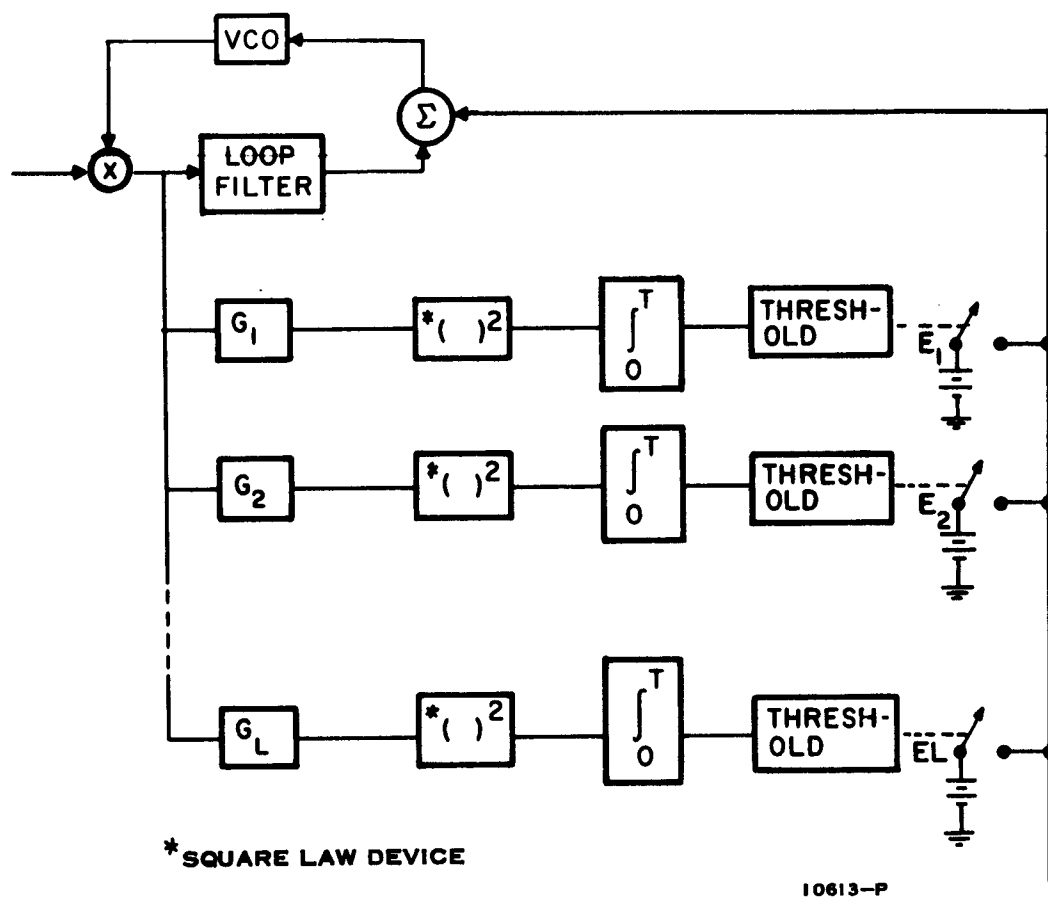


Fig. 3-5 The Optimum Receiver

SECTION 4

INTERFERENCE TO A TRACKING LOOP FROM AN UNWANTED CARRIER
(WITH LIMITING)

SECTION 4

INTERFERENCE TO A TRACKING LOOP FROM AN UNWANTED CARRIER
(WITH LIMITING)

4.1 GENERAL

An interfering signal affects a phase-locked loop in much the same way such a signal would affect a standard F-M discriminator. When the interfering carrier is slightly stronger than the wanted signal, there is complete capture by the interference. When the interference is less than the wanted signal, the tracking range is reduced. Thus, the phase-locked loop is not ideally suited to a secure communication system.

The following practical example is the simplest possible - a friendly and an unfriendly carrier, both of which are unmodulated. This example will serve to illustrate the concepts involved in more complicated cases. An understanding of these concepts is perhaps all that is necessary, because there is little the designer of the loop can do (other than use perfect integration or use the narrowest possible loop) to combat coherent interference.

Since the output of an ideal limiter is purely phase modulated, the equivalent input to the linear loop will be this phase modulation. The phase may be found by solving for θ in Fig. 4-1. Solving for the phase, E_1 is the signal amplitude and E_2 is the interfering amplitude. E_2 in Fig. 4-1 rotates at the beat frequency.

$\theta(t)$ is shown in Fig. 4-2 for $E_2/E_1 = 0.6$. Since it is plotted as an odd function, $\theta(t)$ may be expressed as a Fourier Series in sine terms only. Table 4-1 shows the coefficients of the first several sine terms for various ratios of E_2 to E_1 .

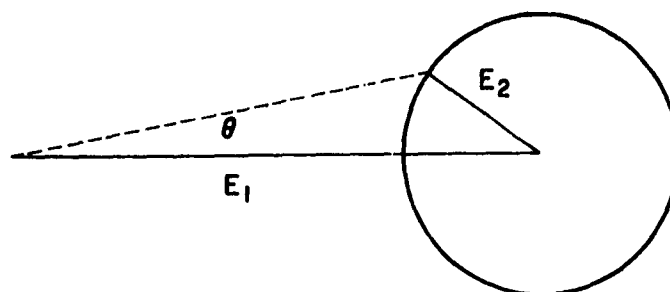


Fig. 4-1 Solving for the Input Phase--with Limiting

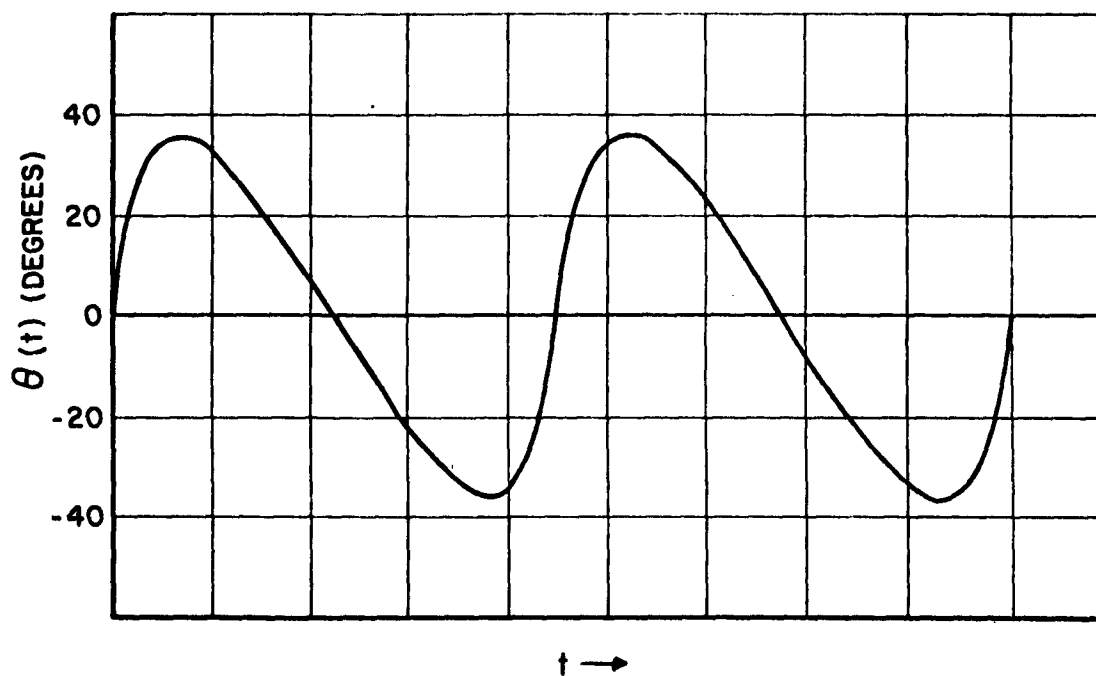
Fig. 4-2 Input Phase as a Function of Time
($E_2/E_1 = 0.6$)

TABLE 4-1
FOURIER COEFFICIENTS OF $\theta(t)$

$\frac{E_2}{E_1}$	B_1	B_2	B_3	B_4	B_5
0.2	0.2019	0.02115	0.00175	0.00101	0.00047
0.4	0.3992	0.08011	0.02152	0.00453	0.00112
0.6	0.5931	0.1763	0.06807	0.02923	0.01073
0.8	0.7882	0.3084	0.1553	0.08161	0.03742
1.0	0.9758	0.4513	0.2597	0.1491	0.06899

Notice that for $E_2/E_1 < 0.6$, the harmonics are small compared to the fundamental. For a first approximation, the phase modulation may be considered sinusoidal with amplitude B_1 .

For $E_2/E_1 > 0.6$, the second and third harmonic must be included. Then the phase error due to the interfering carrier may be calculated by the methods of Section 2; i.e., use Equation (3) to obtain

$$|e_o(t)|_{\max} = \frac{B_1 \omega_o}{j\omega_o + K_{OL} G(j\omega_o)} \quad (4-1)$$

where ω_o is the beat frequency and $e_o(t)$ is the error due to the interference (the analysis so far applies to either a modulated or an unmodulated friendly signal). The interference error $e_o(t)$ will be riding on the phase error caused by the doppler shift (or modulation). The absolute value of the doppler error plus $e_o(t)_{\max}$ must be less than 90 degrees; obviously, the larger $e_o(t)_{\max}$, the smaller the tracking range.

Figure 4-3 shows a typical root locus that may be used to solve Equation 4-1.

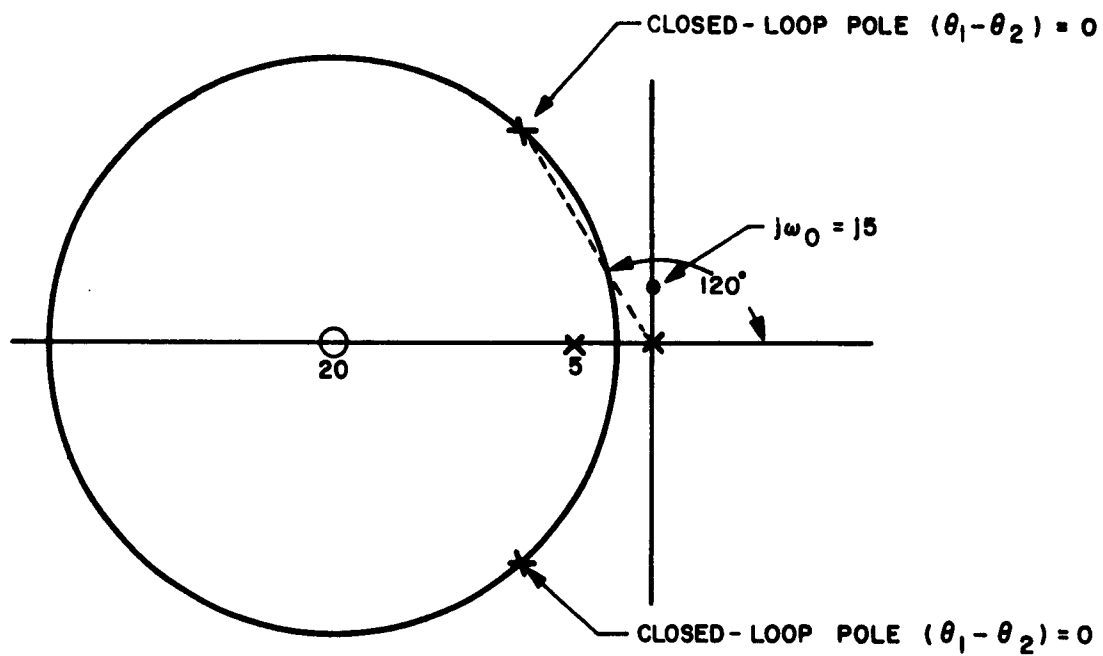


Fig. 4-3 A Typical Root Locus for Finding the Maximum Phase Error

It has been shown that the small-signal open-loop gain K_{OL} is proportional to $\cos(\theta_1 - \theta_2)$. First, find the zero-error K_{OL} and using this value calculate $|e_o(t)|_{\max}$ for the zero error, using loop pole positions corresponding to K_{OL} . Then multiply K_{OL} by $\cos\left[\frac{\pi}{2} - |e_o(t)|\right]$ to obtain a new value of K_{OL} (the loop can track out to $\frac{\pi}{2} - |e_o(t)|_{\max}$, so K_{OL} must be calculated for this entire region). New closed-loop pole positions are then found, and a new $|e_o(t)|_{\max}$ is determined. This iterative process is continued until it is obvious that there is convergence to the proper value of $|e_o(t)|_{\max}$. When second and third harmonics are used, the relative phase shifts at each of the three frequencies should be noted. The three components can then be easily combined to obtain $|e_o(t)|_{\max}$. Once they have been determined for the fundamental, no readjustment of the closed-loop poles is necessary. This $|e_o(t)|$ subtracted from $\pi/2$ is a good estimate of the tracking limit for the given ω_o and E_2/E_1 .

Figure 4-4 shows the decrease in tracking range with an increase in E_2/E_1 for the loop of Fig. 4-3 and an ω_o of 5. This curve is quite typical of most phase-locked loops where the beat frequency is small in comparison with the loop bandwidth.

In many practical cases, both ω_o and E_2/E_1 are varying continuously. Although no general curve can be drawn, a family of curves may be drawn using the above procedure, and from this family the desired information may be obtained.

Because the "no noise" limits are lowered, the noise thresholds are raised. Since the noise from the limiter is not Gaussian, no attempt has been made to calculate this change in threshold. It is likely that, as an order of magnitude, the threshold will increase by a factor of

$$\frac{\pi/2}{\frac{\pi}{2} - |e_o(t)|_{\max}}$$

Probably the actual interference will be more bothersome than the increase in the threshold level.

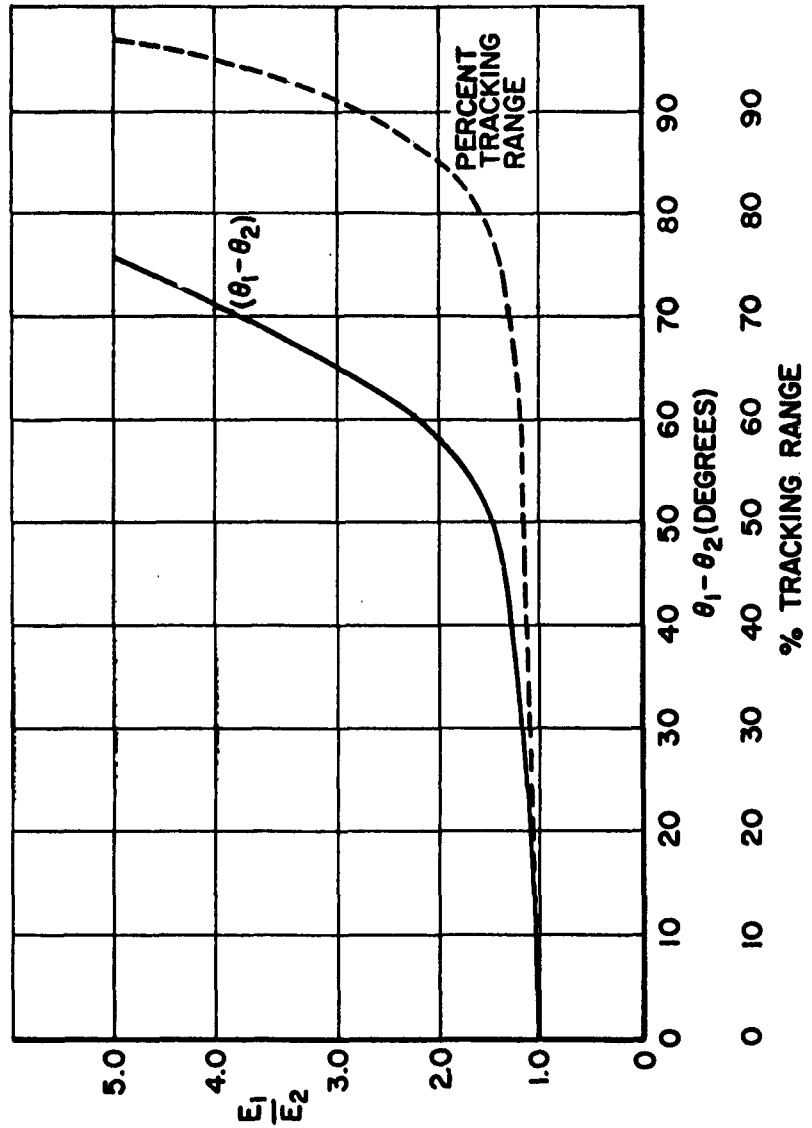


Fig. 4-4 Calculated Signal-to-Interference Threshold ---
with Limiting

REFERENCES

Newton, G. C.; L. A. Gould and J. F. Kaiser, Analytical Design of Linear Feedback Controls, New York, N. Y., John Wiley Sons, Inc., p. 371, 1957

Stumpers, F. L. H. M., "Theory of F.M. Noise, "Proceedings of the IRE, p. 1086, September, 1948

Weaver, C. S., WDL-TR1334, Preliminary Studies of Adaptive Processes Applied to Phase-Locked Loops," Philco Western Development Laboratories, p. 3, 15 September 1960.

Weaver, C. S., WDL-TR1447, Thresholds and Tracking Ranges in Phase-Locked Loops, Philco Western Development Laboratories, p. 19, 15 April 1961

APPENDIX A
DOPPLER LOOP THRESHOLD

APPENDIX A DOPPLER LOOP THRESHOLD

A.1 THRESHOLD OPTIMIZATION

The threshold of a phase-locked loop may be optimized by minimizing the probability of the phase error exceeding some limit (usually $\pi/2$). To do this, one may consider the phase error as a random variable with a mean μ equal to the peak instantaneous phase error due to transients in the loop as it follows the signal carrier (and modulation, if applicable). The variance, σ^2 , of the random variable will be the phase noise power at the output of the VCO.

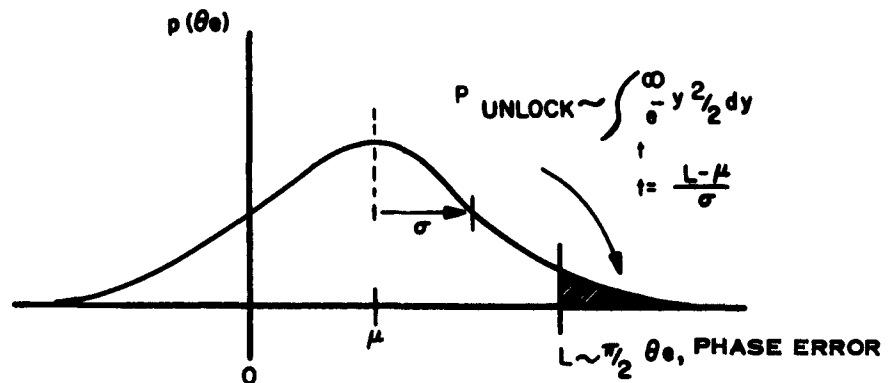


Fig. A-1 Distribution of Phase Error

In a doppler tracking loop, with an integrating filter, the instantaneous phase error due to signal transients in the loop is a constant proportional to the drift rate, $\dot{\omega}$. Specifically $\mu = \dot{\omega}/\omega_n^2$.

The variance is found from the noise density at the input to the detector, N_o , the actual noise bandwidth (see Fig. 1-5) and the peak signal amplitude of the incoming sine wave, E_s .

$$\begin{aligned}\sigma^2 &= N_o \times \text{B.W.} \times R \times \frac{1}{2E_s^2} \\ &= \frac{N_o}{4E_s^2} W_n\end{aligned}$$

To minimize the probability of the loop falling out of lock is equivalent to minimizing the shaded area of Fig. A-1. This may be accomplished by maximizing the normalized standard deviation, t .

The usual rules of the calculus are as follows:

$$\begin{aligned}t &= \frac{1 - \mu}{\sigma} \\ &= \sqrt{\frac{4E_s^2}{N_o}} \frac{L \omega_n^2 - \dot{\omega}}{\omega_n^{5/2}} \\ \frac{\partial t}{\partial \omega_n} &= \sqrt{\frac{4E_s^2}{N_o}} \frac{5\dot{\omega} - \omega_n^2 L}{2 \omega_n^{7/2}} = 0 \\ \omega_n &= \sqrt{\frac{5}{L} |\dot{\omega}|}\end{aligned}$$

A check of the second derivative evaluated at this value of ω_n verifies that it represents a maximum in t .

One implied assumption is that the relative bandwidth, R , can be held constant as ω_n is varied to the optimum. This means that the pole-zero configuration must maintain symmetry as ω_n is adjusted.

An interesting conclusion is that while the actual threshold is affected by the signal power to noise density ratio, the choice of optimum bandwidth is dependent only on the drift rate.

A.2 AN ALTERNATE FORMULATION

An alternate approach considers the effect of the second tail of the probability distribution. An assumption is made that the area of each tail of the distribution is proportional to the reciprocal of the normalized standard deviation. The minimization of the area thus defined resulted in an answer similar to the first method:

$$\omega_n = \sqrt{\frac{3}{L} |\dot{\omega}|}$$

DISTRIBUTION LIST

<u>Address</u>	<u>No. of Copies</u>
Commander Space Systems Division Air Force Systems Command Air Force Unit Post Office Los Angeles, California Attn: Technical Data Center	10
USAF Contract Support Detachment No. 3 Philco Corporation Western Development Laboratories Palo Alto, California	1
Philco Corporation Western Development Laboratories Palo Alto, California	89 + 1 reproducib
Philco Corporation Plant 50 4700 Wissahickon Ave. Philadelphia 44, Pennsylvania Attn: D. Kinnier (Engineering)	1
Philco Corporation Plant 37 Union Meeting Road Blue Bell, Pennsylvania Attn: R. Murphy	1
Philco Corporation Computer Division 3900 Welsh Road Willow Grove, Pennsylvania Attn: Librarian	1
	<hr/> 103 + 1 reproducib

PHILCO